الجمهورية الجزائرية الديمقراطية الشعبية
République algérienne démocratique et populaire
وزارة التعليم العالي والبحث العلمي
Ministère de l'enseignement supérieur et de la recherche scientifique
جامعة عين تموشنت بلحاج بوشعيب
Université –Ain Temouchent- Belhadj Bouchaib
Faculté des Sciences et de la Technologie
Département : Génie mécanique

Projet de Fin d'Etudes
Pour l'obtention du diplôme de Master en : Génie des Procédés
Domaine : Sciences et de la Technologie
Filière : Génie des Procédés
Spécialité : Génie des Procédés des matériaux
Thème

PRODUCTION OF HYDROGEN

Présenté Par :

Mr. MIZHA Martin Farai

Soutenu le 02/06/2025 devant le jury composé de :

Mme. Younes Kawther	Dr. UAT.B.B (Ain Temouchent)	Président
Mr. REMLAOUI Ahmed	Dr. UAT.B.B (Ain Temouchent)	Examinateur
Mr. NEHARI Driss	Prof. UAT.B.B (Ain Temouchent)	Encadreur
Mme. BEKRAOUI Hafsa	Dr. UAT.B.B (Ain Temouchent)	Co-Encadreur

Année Universitaire 2024/2025

Remerciements

Tout d'abord, je tiens à manifester ma louange et ma gratitude à Dieu pour sa grâce et son excellence en me donnant la volonté, la santé et la patience d'achever ce travail. Je tiens à exprimer ma profonde gratitude à mon directeur de mémoire, Prof. Nehari Driss, pour ses précieux conseils, son soutien et son encouragement tout au long de ce projet. Son expertise, sa patience et ses remarques constructives ont joué un rôle déterminant dans la réussite de ce travail. Une reconnaissance toute particulière va également à Mme. Bekraoui Hafsa, en tant que co-encadreur, pour son travail sans relâche aux côtés de Monsieur Nehari, contribuant ainsi au succès de ce projet.

Je remercie également les membres du jury d'avoir pris le temps d'évaluer mon travail Dr. Younes Kawther, Président du jury et Dr. Remlaoui Ahmed, l'examinateur. C'est un grand honneur des les avoir commes de ce projet.

Je souhaite également exprimer ma reconnaissance à l'ensemble des professeurs et du personnel du Département Génie des Procédés pour le savoir et le soutien apportés tout au long de mon parcours académique. Un grand merci à mes collègues et amis pour leur collaboration et leur soutien.

Enfin, je suis profondément reconnaissant à ma famille pour son soutien indéfectible, son amour et sa confiance tout au long de mes études.

Abstract

This study provides a systematic evaluation of hydrogen production methods, with focus on optimizing solar-powered alkaline electrolysis for sustainable energy systems. While analyzing conventional pathways (steam reforming, pyrolysis) and emerging alternatives (PEM/SOEC electrolysis), the research identifies alkaline electrolyzers as the most viable technology for large-scale solar hydrogen in high-irradiation regions like Algeria. Through MATLAB simulations validated by PVGIS data, we demonstrate how 80°C operation improves electrolyte conductivity (115.5 S/m) while managing overpotentials (total cell voltage: 2.24 V). Practical implementation challenges are addressed through: (1) sensitivity analysis of Faradaic/PV efficiencies, (2) comparative assessment of storage/transport methods, and (3) levelized cost modeling (€4.50/kg at optimized conditions). The work bridges theoretical principles with deployable solutions, offering actionable insights for renewable hydrogen projects in sun-rich developing economies.

Keywords: Hydrogen Production Methods, Alkaline Water Electrolysis, Solar-to-Hydrogen Efficiency, Techno-Economic Analysis, Renewable Hydrogen Storage.

Resume

Cette étude propose une évaluation systématique des méthodes de production d'hydrogène, en se concentrant sur l'optimisation de l'électrolyse alcaline alimentée par l'énergie solaire pour des systèmes énergétiques durables. Tout en analysant les méthodes conventionnelles (vaporeformage, pyrolyse) et les alternatives émergentes (électrolyse PEM/SOEC), la recherche identifie les électrolyseurs alcalins comme la technologie la plus viable pour la production à grande échelle d'hydrogène solaire dans les régions à fort ensoleillement comme l'Algérie. Grâce à des simulations MATLAB validées par des données PVGIS, nous démontrons qu'une opération à 80°C améliore la conductivité électrolytique (115,5 S/m) tout en gérant les surpotentiels (tension totale de cellule : 2,24 V). Les défis pratiques sont abordés via : (1) l'analyse de sensibilité des rendements Faradaïque/PV, (2) l'évaluation comparative des méthodes de stockage/transport, et (3) la modélisation des coûts actualisés (4,50 €/kg dans des conditions optimisées). Ce travail relie les principes théoriques aux solutions déployables, offrant des insights actionnables pour les projets d'hydrogène renouvelable dans les économies ensoleillées en développement.

Mots clés: Méthodes de production d'hydrogène, Électrolyse alcaline de l'eau, Efficacité solaire-hydrogène, Analyse technico-économique, Stockage d'hydrogène renouvelable.

Table of Contents

Chapter 3: Results and Discussion

LIST OF FIGURES

LIST OF TABLES

0 General Introduction

As the global demand for energy continues to grow, humanity faces the pressing challenge of transitioning from fossil fuel dependency to sustainable, low-carbon energy systems. The combustion of fossil fuels, which has historically driven industrial development, is now recognized as a major contributor to greenhouse gas emissions and environmental degradation. This has prompted an urgent search for alternative energy carriers that are both clean and efficient. In this context, hydrogen has emerged as a promising candidate. Owing to its high energy content per unit mass and its ability to produce only water as a by-product when used, hydrogen is widely regarded as a key enabler of the global energy transition.[1]

However, hydrogen does not occur naturally in its molecular form and must be produced through various chemical or electrochemical processes. These production methods can be broadly classified into two categories: non-renewable and renewable. Non-renewable methods, such as steam methane reforming, coal gasification, and partial oxidation, dominate current global hydrogen production but are associated with significant carbon emissions. In contrast, renewable hydrogen production pathways, including biomass gasification, photo-electrochemical water splitting and water electrolysis powered by renewable electricity, offer the potential to decouple hydrogen production from fossil fuel use [2]. Among these, solar-powered electrolysis presents a particularly attractive route due to the abundant and widely available nature of solar energy, especially in regions such as North Africa, Southern Africa and the Middle East. In Algeria, the production of hydrogen presents a strategic opportunity due to the country's abundant natural gas reserves, high solar energy potential and available biomass resources. With its position as a major exporter of natural gas, Algeria has the capability to develop blue hydrogen (hydrogen produced via natural gas with carbon capture and storage). At the same time, the country's significant solar potential makes green hydrogen via electrolysis an attractive long-term solution.

Despite its advantages, solar hydrogen production via electrolysis faces several technical and economic challenges. The high capital costs of photovoltaic and electrolysis systems, coupled with inefficiencies in energy conversion and hydrogen generation, pose significant barriers to large-scale deployment. Therefore, research efforts have increasingly focused on identifying and optimizing the key parameters that influence the performance and cost-effectiveness of these systems[3]. By simulating and evaluating various design configurations and operating conditions, it is possible to gain insights that guide the development of more efficient, economically viable hydrogen production systems.

This thesis contributes to this field of research by first providing a comprehensive overview of hydrogen production methods, with an emphasis on their environmental impact and suitability for integration with renewable energy. Building on this foundation, the focus shifts to solar-powered electrolysis, where both the technology and associated optimization strategies are reviewed in detail. A MATLAB-based simulation is then developed to model a PV-electrolysis system under

real environmental conditions. Two cases are presented: a baseline model using standard assumptions, and an optimized model where selected parameters, such as Faradaic efficiency, electrolyte conductivity, electrode spacing and PV efficiency are systematically varied to assess their impact on hydrogen yield and production cost.

The structure of this thesis reflects this logical progression. Chapter 1 introduces the fundamentals of hydrogen production and renewable energy systems, providing a theoretical basis for the study. Chapter 2 presents a detailed review of hydrogen production technologies, with a specific focus on solar-powered electrolysis and the various approaches used to enhance system performance. Chapter 3 presents the modelling and simulation work, highlighting the influence of design and operational parameters on both technical and economic outcomes. Through this work, the thesis aims to contribute practical insights into the development of optimized, cost-effective systems for green hydrogen production, particularly relevant for sun-rich regions like Algeria and beyond.

1 Chapter 1: Fundamentals of Hydrogen Production

1.1. Introduction

Hydrogen is increasingly recognized as a key energy carrier in the global transition toward cleaner and more sustainable energy systems. Its versatility allows it to serve multiple roles, from industrial feedstock to fuel for transportation and electricity generation. However, producing hydrogen in an environmentally and economically sustainable way requires a solid understanding of the underlying physical, chemical, and energy systems involved.[2]

This chapter lays the theoretical foundation necessary to understand and model hydrogen production systems, especially those powered by renewable energy. It begins by outlining the essential physical and chemical properties of hydrogen, emphasizing its energy content, storage characteristics, and behaviour as a fuel. The discussion then shifts to the fundamentals of renewable energy systems, highlighting how sources like solar and wind can provide clean power for hydrogen generation. A particular focus is given to photovoltaic (PV) systems due to their central role in the simulation work presented later in this thesis.

In addition, the chapter introduces the principles of water electrolysis, which is the core technology for converting renewable electricity into hydrogen. Rather than detailing specific technologies at this stage, the focus remains on general electrochemical principles and system-level considerations. The chapter concludes by exploring the conceptual integration of PV systems with electrolysis, setting the stage for the deeper technology review and optimization strategies discussed in Chapter 2.

1.2. History of Hydrogen

The scientific journey of hydrogen began in earnest with 17th-century alchemists observing flammable gas from metal-acid reactions, though it was Henry Cavendish's 1766 systematic experiments that first isolated and characterized what he termed "inflammable air." Lavoisier's 1783 nomenclature ("hydrogène") and quantitative demonstration of water formation established hydrogen's fundamental chemical identity while providing the first stoichiometric understanding of gas production through acid-metal reactions[4], [5]. The Industrial Revolution transformed hydrogen from laboratory curiosity to commercial commodity, with coal gasification plants (early 1800s) producing "town gas" (containing 50% hydrogen) for urban lighting - an infrastructure later repurposed for industrial hydrogen needs. Simultaneously, Nicholson and Carlisle's 1800 demonstration of water electrolysis established an alternative production pathway, though its prohibitive energy costs limited adoption until the late 19th century advent of hydroelectric power enabled the first commercial electrolysers in Norway (1890s) for fertilizer[5]. The 20th century witnessed hydrogen's industrialization through three parallel tracks the 1913 Haber-Bosch process's massive ammonia demand drove steam reforming of hydrocarbons (initially coal, later natural gas); the 1920s alkaline electrolyser developments supported niche applications requiring high-purity hydrogen (e.g., metallurgy, electronics); and wartime needs (1930s-40s) accelerated large-scale liquefaction and handling technologies. The post-war era cemented steam methane reforming (SMR) as the dominant production method (now ~95% of supply) due to its

thermodynamic efficiency (70-85%) and integration with petroleum refining, though with growing recognition of its carbon intensity (12 kg CO_2/kg H_2) [6]. Environmental regulations and oil crises (1970s) revived interest in electrolysis, spurring advances in solid polymer (General Electric, 1960s) and solid oxide electrolysis cells (1980s) that achieved efficiencies surpassing 75%. Contemporary hydrogen production stands at an energy transition crossroads. While SMR with carbon capture (blue hydrogen) offers near-term decarbonisation, renewable-powered electrolysis (green hydrogen) has seen costs plummet from ~$20/kg (1980) to $3-6/kg today through PEM technology scaling and renewable electricity price declines [3]. Emerging methods like photo-electrochemical (2010s) and microbial production (2000s) remain in R&D but promise solar-to-hydrogen efficiencies beyond 10%. The EU's 2×40 GW electrolyser target (2030) and U.S. Inflation Reduction Act's $3/kg production tax credit exemplify policy drivers reshaping production economics, though challenges persist in renewable integration, durability (>80,000h for PEM stacks), and supply chain scaling [7].

1.3. Properties of Hydrogen

Property	Value
Molecular weight [g/mol]	2.016
Density [g/L]	0.08988
Boiling Point [°C]	-252.87
Melting Point [°C]	-259.16
Critical Temperature [°C]	-240.17
Critical Pressure [atm]	12.97
Triple Point [°C], [kPa]	-259.35°C, 7.042kPa
Specific Heat Capacity [J/g.K]	14.267
Heat of Vaporization [kJ/mol]	0.449
Thermal Conductivity [W/m.K]	0.1805
Viscosity [Pa.s]	$8.76*10^{-6}$
Solubility in Water [mg/L]	1.6
Flammability Limits in Air [%volume]	4.0-75.0
Auto-Ignition Temperature [°C]	500-585
High heating value 'HHV' [MJ/kg]	141.9
Low heating value 'LHV' [MJ/kg]	119.9

Table 1.1: Physical Properties of Hydrogen [4], [8]

Property	Value/Description	Notes
Molecular Formula	H_2	Diatomic molecule
State at rtp	Colourless, ordoless gas	-
Bond Energy (H-H) [kJ/mol]	436	-
Oxidation States	+1(in compounds), 0(elemental)	-
Reactivity	Highly flammable, reduces metals	Forms Hydrides (e.g NaH)
Isotopes	Protium(^1H), Deuterium(^2H), Tritium(^3H)	Tritium is radioactive
Electronegativity	2.20	-
Standard Electrode Potential	0.00	V for $2H^+ + 2e^-$ ➔ H_2
Common Reactions	Combustion: $2H_2 + O_2$ ➔$2H_2O$ Metal Reduction: *for example*: $CuO + H_2$ ➔$Cu + H_2O$	Exothermic reactions

Table 1.2: Chemical Properties of Hydrogen [9]

1.3.1. Analysis of Hydrogen Properties Related to Use and Storage

- Low Density (0.0899 kg/m³ at STP): Hydrogen has the lowest density of all gases, making it challenging to store compactly. This necessitates high-pressure tanks, cryogenic storage, or conversion to other carriers like ammonia or methanol for volume-efficient transport and storage. [4]

- Small Molecular Size: Due to its tiny molecular structure, hydrogen can easily diffuse through materials, leading to potential leakage issues. This demands the use of special materials and seals in pipelines and storage vessels.

- High Flammability and Wide Flammability Range (4–75% in air): While its flammability enables its use as a fuel, it also poses safety concerns, especially in enclosed environments. Strict safety measures are essential during storage and transportation.

- Low Boiling Point (-252.87°C): Cryogenic storage of liquid hydrogen requires advanced insulation systems and contributes to high energy costs during liquefaction.[10]

- High Energy Content per Unit Mass (120–142 MJ/kg): Hydrogen offers three times more energy per kg than gasoline, making it very attractive for fuel applications, particularly in

aviation and space. However, its low energy per unit volume requires innovations in storage systems. [8]

1.4.Advantages and Challenges[11]

As hydrogen gains prominence as a clean energy carrier, it is essential to evaluate both the strengths that make it an attractive solution and the limitations that hinder its widespread adoption. This section presents a balanced view of hydrogen's key advantages and the technical, economic, and safety-related challenges that must be addressed to enable its full integration into modern energy systems.

The advantages include:

- When used in fuel cells, hydrogen produces electricity with water and heat as the only by-products, making it a clean and environmentally friendly energy source.
- Hydrogen can be used in a variety of applications, including transportation, electricity generation, and industrial processes.
- Hydrogen has a high energy content per unit of mass, making it a potentially efficient energy carrier.
- Hydrogen produced through electrolysis using renewable energy sources can help to reduce greenhouse gas emissions, especially if it replaces fossil fuels in various sectors.
- Hydrogen can serve as an effective means of storing excess energy generated from intermittent renewable sources, helping to address the issue of energy storage.

The challenges entail:

- Most hydrogen is currently produced from natural gas in a process called steam methane reforming, which emits carbon dioxide.
- Hydrogen has low energy density by volume, which makes storage and transportation challenging. It requires specialized infrastructure and technologies to handle and transport it efficiently.
- Hydrogen production, especially from renewable sources, can be expensive.
- The process of converting hydrogen back into electricity in fuel cells involves energy losses, and the overall efficiency of hydrogen energy systems may be lower than that of some other energy sources.
- Hydrogen is highly flammable and has a wide flammability range. Special safety measures and technologies are required for handling, storage, and transportation to minimize the risks.

- While hydrogen is abundant in the universe, it is rarely found in its elemental form on Earth. It is typically bound to other elements and extracting it can be energy intensive.

1.5. Uses of Hydrogen

1.5.1. Hydrogen as an Industrial Reactant

Hydrogen is widely used in industries where it reacts directly with other substances or is integrated into manufacturing processes.

- Ammonia production for fertilizers

Hydrogen reacts with nitrogen in the Haber–Bosch process to produce ammonia (NH_3), which is essential for agricultural fertilizers. This is currently the largest use of hydrogen globally, accounting for about 50% of the total hydrogen used all over the world.[2], [10]

- Oil refining and fuel upgrading

Used in hydrocracking and hydrotreating to remove sulphur and break down heavier crude oil components into cleaner fuels like gasoline and diesel.[2], [12]

- Methanol and synthetic chemical production

Hydrogen can be combined with carbon monoxide or carbon dioxide to make methanol, a building block for plastics, formaldehyde and acetic acid. Hydrogen also enables production of synthetic hydrocarbons and e-fuels.[2], [10]

- Hydrogenation of organic compounds

It is applied in chemical industries to saturate organic compounds (e.g., converting unsaturated fats to margarine) and in the manufacture of pharmaceuticals and food products.[12]

- Steel and iron production (Direct Reduction)

It works as a replacement for carbon-based agents like coke in steelmaking through hydrogen-based direct reduction, producing only water vapour instead of CO_2.[10], [12]

- High-purity applications in electronics

At an industrial level, hydrogen is also used in controlled environments to produce semiconductors, fibre optics and flat-panel displays due to its high purity and inert characteristics.[12]

1.5.2. Hydrogen as an Energy Carrier and Storage Vector

- Grid energy storage and Power generation

Hydrogen is used as a medium to store excess electricity generated from renewable sources. During times of low energy generation, the stored hydrogen can be converted back to electricity using fuel cells or turbines. This enables clean backup power, off-grid systems, and even centralized generation with zero carbon emissions.[2]

- Production of synthetic fuels (power-to-liquids)

Hydrogen reacts with captured CO_2 to produce synthetic liquid fuels (e.g., e-diesel, e-kerosene), offering a carbon-neutral alternative for sectors that are hard to electrify.

- Energy transport across borders

Hydrogen can be compressed, liquefied, or converted to carriers like ammonia for easier storage and long-distance export/import between regions with different renewable capacities.[2]

1.5.3. Hydrogen for Sustainable Mobility and Transport

Hydrogen offers clean propulsion for a wide range of transport modes, especially where batteries are heavy, slow to charge, or unsuitable.

- Fuel Cell Electric Vehicles (FCEVs)

Vehicles powered by hydrogen fuel cells emit only water vapour. They offer faster refueling and longer range than battery electric vehicles, especially in taxis, buses and commercial fleets.[10]

- Heavy-duty and long-range vehicles

Trucks, long-distance buses, and delivery vans benefit from hydrogen's high energy density, making it suitable for logistics and freight sectors. In railways where installing electric overhead lines is expensive or impractical, the use of hydrogen comes as a tangible solution. Hydrogen trains are already operating in parts of Europe.[2], [10]

- Maritime shipping

Hydrogen and its derivatives like ammonia or methanol can fuel ships, reducing emissions in global marine transport.[10]

- Future potential in aviation

Hydrogen is being explored for direct combustion in aircraft engines and for producing synthetic aviation fuels to meet decarbonization targets.[10]

1.5.4. Hydrogen for Heat and Thermal Applications

Hydrogen can be used directly to generate heat in industrial and residential settings, displacing natural gas and coal.

- Industrial process heat

Provides high-temperature heat (>1000°C) required in industries like cement, glass, steel, and ceramics, where electrification is difficult or inefficient.[12]

- Hydrogen boilers for residential and commercial heating

Hydrogen can be blended with natural gas or used alone in modified boilers to provide heat for homes and buildings.[10]

- District heating and combined heat and power (CHP)

Hydrogen may be integrated into district heating networks or cogeneration systems to provide both electricity and heat.[2]

1.6. Hydrogen's Strategic Value in the Energy Transition: Key Roles and Impacts

Importance	Role	Impact
Decarbonizes hard-to-abate sectors	Industrial feedstock (steel, chemicals) replacement	Addresses 30% of global emissions that primary renewables can't fix
Enables renewable energy integration	Long-duration energy storage	Solves intermittency issues of solar/wind at scale
Clean mobility for heavy transport	Trucking, shipping, aviation fuel	Replaces diesel in sectors where batteries fail
Replacing fossil fuels in heating	Gas grid blending *[mixing H_2 with natural gas (methane, CH_4) in existing pipeline networks to reduce carbon emissions from heating and industrial processes*]	Decarbonizes heating (12% of emissions)

Table 1.3: Importance, roles and impacts of H_2

1.7. Hydrogen Production Methods

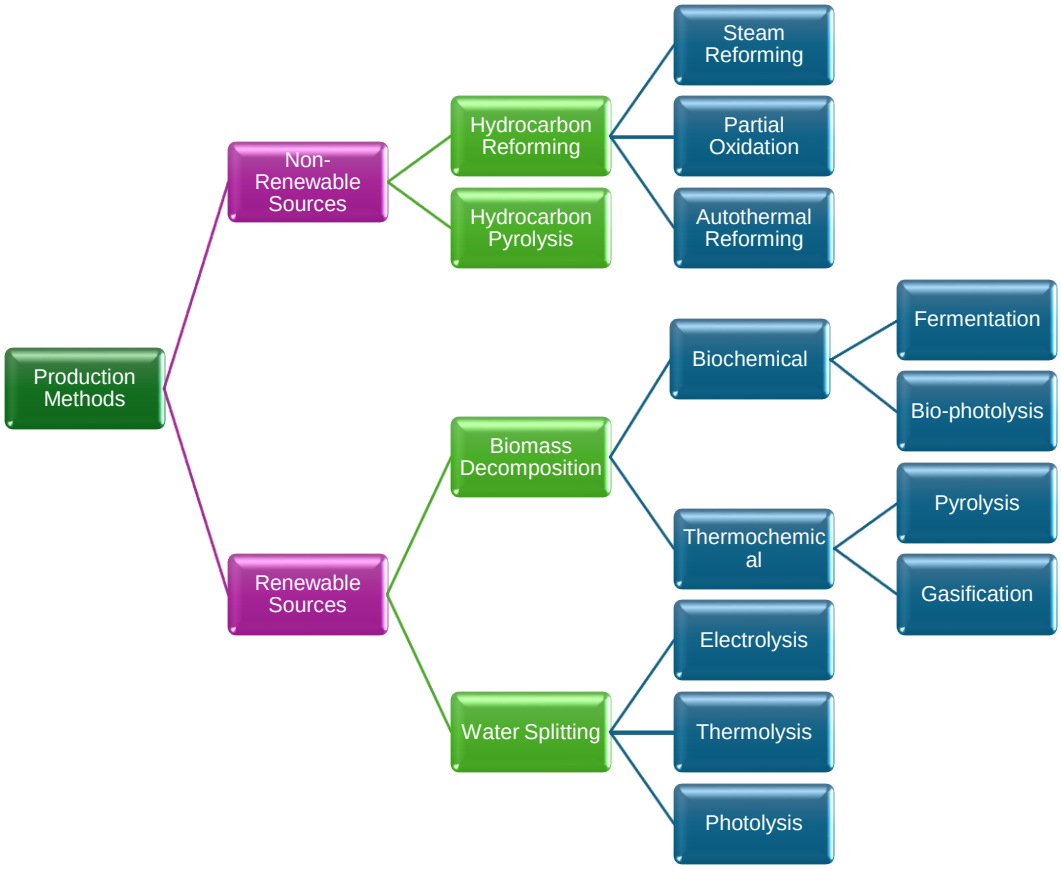

Figure 1.1: Methods of hydrogen production[8], [10]

1.7.1. Hydrogen Production from Non-Renewable Sources

Hydrogen production from non-renewable sources primarily relies on fossil fuels, including natural gas, coal and oil. There are several technologies of producing hydrogen from fossil fuels, the main of which are hydrocarbon reforming and pyrolysis[8]. These methods are widely used due to their cost-effectiveness but contribute to greenhouse gas emissions, necessitating carbon capture technologies for cleaner hydrogen production. According to the International Renewable Energy Agency (IRENA), approximately 47% of global hydrogen is produced from methane (natural gas), 27% from coal and 22% as a by-product from oil refining, totally 96% of hydrogen is produced from fossil fuels. In contrast, low-emission hydrogen, including blue hydrogen (produced from fossil fuels with carbon capture and storage), accounts for less than 1% of global production. [3]

1.7.1.1. Hydrocarbon Reforming Methods

Hydrocarbon reforming is the process by which the hydrocarbon fuel is broken down into hydrogen-rich synthesis gas (syngas) through reactions with steam (Steam Reforming), oxygen (Partial Oxidation), or both (Autothermal Reforming). [8]

1.7.1.1.1. Steam Reforming

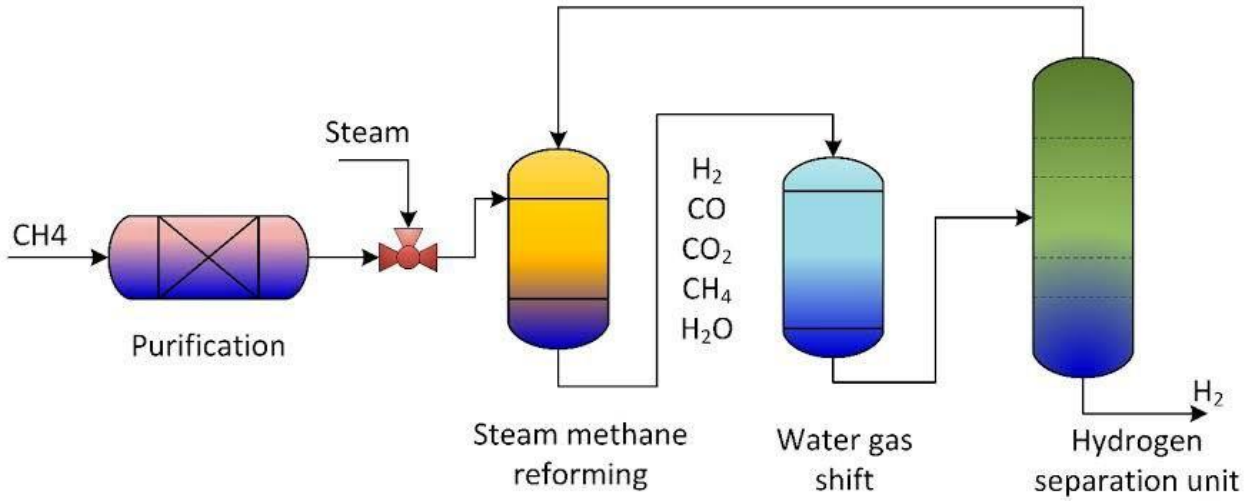

Figure 1.2: SMR process [13]

Basic Principle: Steam reforming is a carbon and energy intensive process that involves converting hydrocarbons and steam into hydrogen and carbon oxides over a catalyst at high temperatures (typically 700–1000°C). [2], [8]

Main Feedstock: The most common feedstock is methane, a light hydrocarbon derived from natural gas, making the process often referred to as Steam Methane Reforming (SMR). SMR is the most advanced and the most widely used industrial process for producing hydrogen from natural gas resources. [10]

Steps involved in the process:

Reforming / Syngas Generation: Methane reacts with steam over a nickel-based catalyst to produce carbon monoxide (CO) and hydrogen (H_2).

Water-Gas Shift (WGS) Reaction: CO from the first step reacts with more steam to yield additional hydrogen and carbon dioxide (CO_2).

Purification: Final hydrogen purification is achieved using pressure swing adsorption (PSA) or methanation to remove remaining CO.

Desulfurization: If the hydrocarbon feedstock contains sulphur compounds, a pre-treatment step is necessary to remove sulphur and prevent catalyst poisoning.[8]

The main chemical reactions that take place in SR are:

Reformer: $C_nH_m + nH_2O \rightarrow nCO + (n + \frac{1}{2}m)H_2$

WGS reactor: $CO + H_2O \rightarrow CO_2 + H_2$

Methanator: $CO + 3H_2 \rightarrow CH_4 + H_2O$ [8]

Advantages and Challenges: SR is mature and cost-effective for large-scale hydrogen production, but it remains carbon-intensive unless coupled with Carbon Capture and Storage (CCS) technologies.[2], [8]

1.7.1.1.2. Partial Oxidation (POX)

Definition: Partial oxidation is a process where a hydrocarbon fuel (like natural gas or diesel) is reacted with a small amount of oxygen, not enough to fully burn it, to produce a gas mixture that contains hydrogen and carbon monoxide. [2], [8]

Raw materials: POX can handle heavy and low-quality fuels like naphtha, diesel, residual oil, or even coal-derived liquids. This makes it useful when cleaner fuels like methane aren't available.[10]

This process has two types, Catalytic POX and Non-Catalytic POX as illustrated in Figure 1.3 below:

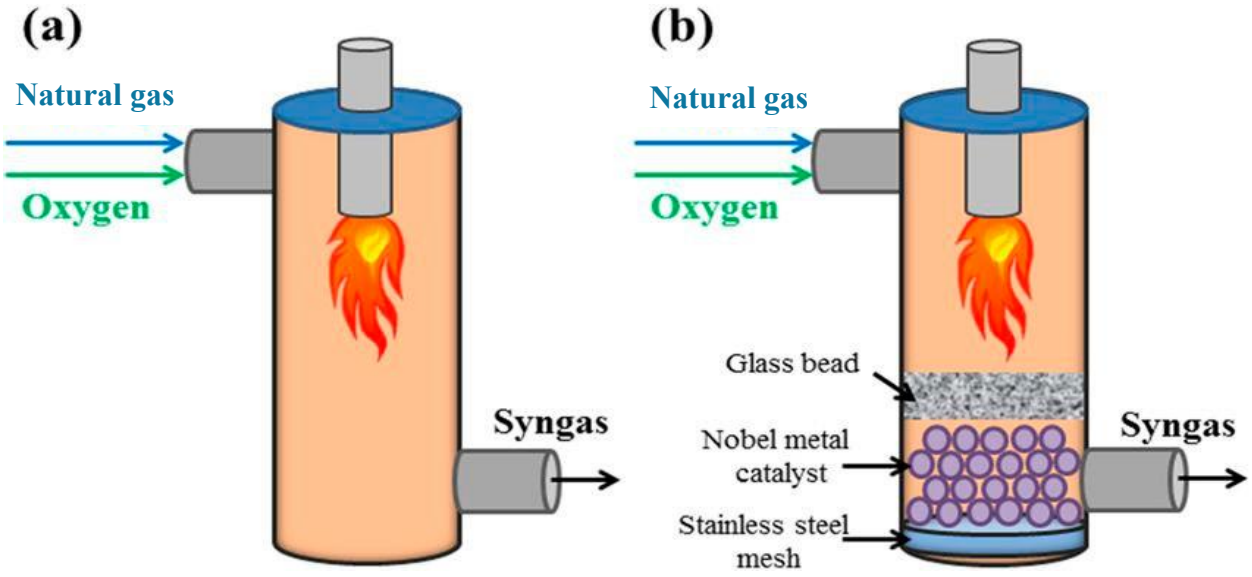

Figure 1.3: (a) Non-catalytic POX reactor and (b) Catalytic POX reactor [14]

Thermal POX: It happens at very high temperatures (1150–1315°C) without a catalyst. It's a simple process but it produces less hydrogen and more unwanted by-products like soot.

Catalytic POX: This process uses a catalyst (like nickel or platinum) to do the reaction at lower temperatures around 950°C. This makes it cleaner and more efficient.

The chemical reactions involved are:

$$Reformer:\ C_nH_m + \frac{1}{2}nO_2 \rightarrow nCO + \frac{1}{2}mH_2 \quad (Catalytic)$$

$$C_nH_m + nH_2O \rightarrow nCO + (n + \frac{1}{2}m)H_2 \quad (Non\text{-}Catalytic)$$

$$WGS\ reactor:\ CO + H_2O \rightarrow CO_2 + H_2$$

$$Methanator:\ CO + 3H_2 \rightarrow CH_4 + H_2O$$ [8]

Advantages: The POX process is faster than steam reforming and the equipment needed is smaller. It can process heavier and dirtier fuels that other methods cannot.

Challenges: It produces less hydrogen than steam reforming. It needs a supply of pure oxygen, which is expensive and requires an air separation unit. [2], [8], [10]

1.7.1.1.3. Autothermal Reforming (ATR)

Definition: ATR is a method that combines features of both steam reforming and partial oxidation in a single reactor. It uses oxygen, steam and a hydrocarbon fuel (like methane or naphtha) to produce hydrogen and carbon oxides.

How it works: First, oxygen partially burns some of the hydrocarbon fuel (a POX reaction), which gives off heat. That heat is then used to support the steam reforming reaction of the rest of the fuel with steam. In other words, ATR method uses the exothermic POX to provide the heat and endothermic SMR to increase the hydrogen production. The two reactions happen together, making the process self-heating, therefore bearing the name, autothermal.

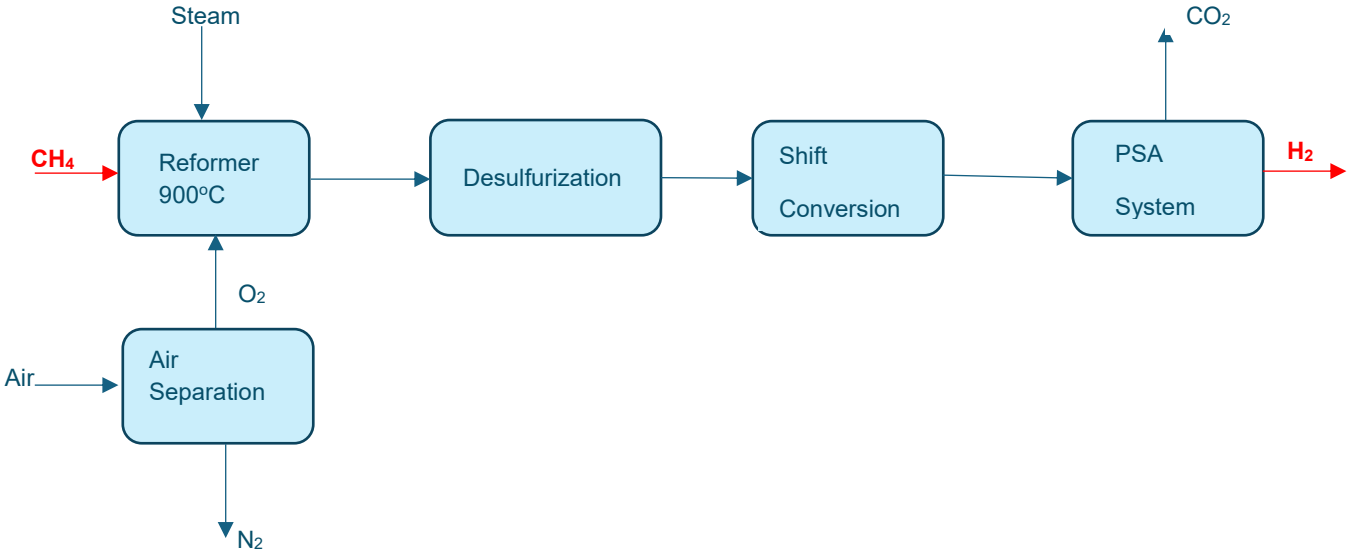

Figure 1.4: Flow diagram of the autothermal reforming of methane [8]

Advantages: It is a more compact and efficient process than separate POX and SR units. This method is well-suited for large-scale hydrogen production, especially when CO_2 capture is added.[8], [10]

Disadvantages: For the operation of ATR, both oxygen and steam are required, which makes the process more complex. The process requires a careful balance between POX and SR to avoid catalyst damage or incomplete reactions.[8]

1.7.1.2. Hydrocarbon Pyrolysis

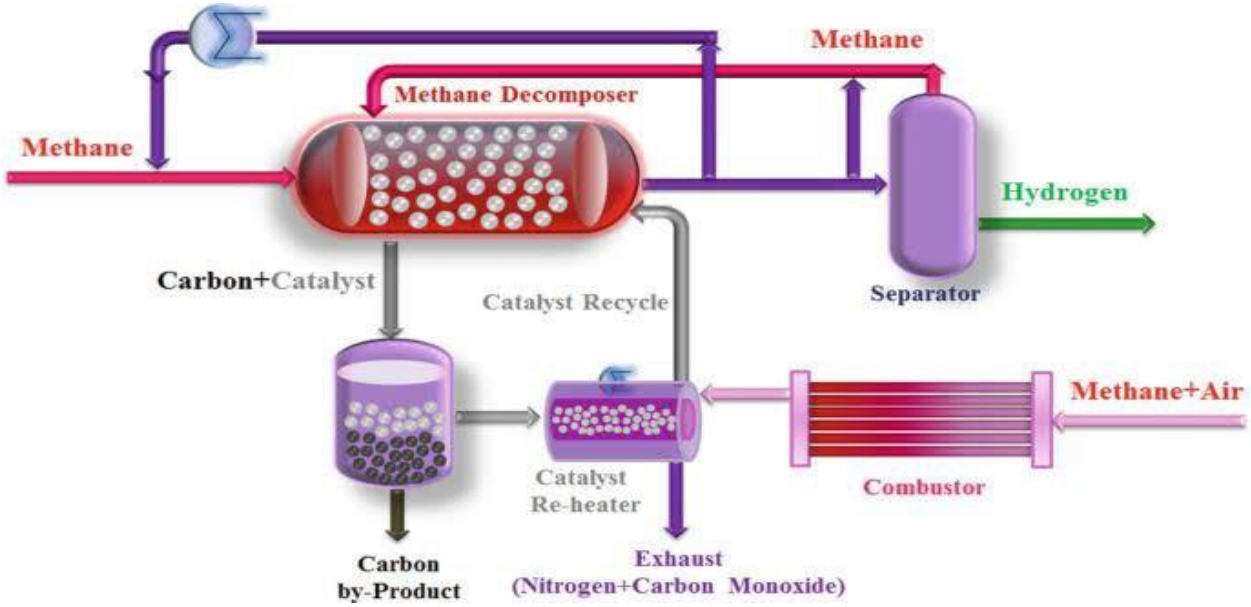

Figure 1.5: The process of hydrocarbon pyrolysis [15]

Definition: Hydrocarbon pyrolysis is a process where methane or other hydrocarbons are broken down at high temperatures in the absence of oxygen to produce hydrogen gas and solid carbon. CO_2 is not directly produced, making this process a promising low-emission hydrogen production method.

The general chemical reaction: $C_nH_m \rightarrow nC + \frac{1}{2}mH_2$

Feedstock and conditions required: The feedstock employed is usually methane, but other hydrocarbons such as propane or heavier fuels can also be used. Requires very high temperatures (around 1000–1200°C) in the absence of air or oxygen (anaerobic conditions) and the use of catalysts is optional, using carbon-based or metal catalysts helps lower the required temperature and improve efficiency. [2], [8], [10]

Advantages: No CO_2 emissions if the carbon is not burned. Solid carbon by-product can have commercial value. Simpler gas treatment since there's no need to remove CO or CO_2.[2]

Challenges: High energy demand due to high temperatures. Carbon build-up may block the reactor or damage the catalyst, so reactor design and carbon removal are important.[2], [8]

1.7.2. Hydrogen Production from Renewable Sources

1.7.2.1. Biomass Decomposition

Hydrogen production from biomass involves converting organic matter such as agricultural residues, forestry waste, and organic municipal waste into hydrogen-rich gas. Since biomass is renewable and absorbs CO_2 during its growth, the overall process can be considered low-carbon or carbon-neutral. The conversion can be achieved through thermochemical or biochemical methods.[10]

1.7.2.1.1. Thermochemical Methods

Thermochemical processes rely on the application of heat to convert biomass into hydrogen and other energy-rich gases. The two primary approaches are gasification and pyrolysis, both of which break down organic matter in high-temperature environments. These processes generate gas mixtures containing carbon monoxide (CO), methane (CH_4), hydrogen (H_2) and other by-products. The CO and CH_4 fractions can undergo further conversion through steam reforming and the water-gas shift (WGS) reaction, thereby increasing the overall hydrogen yield. Less commonly used thermochemical techniques include combustion and liquefaction. Combustion of biomass releases thermal energy but generates only small amounts of hydrogen, along with undesirable emissions such as CO_2 and particulates, making it environmentally less favourable. Liquefaction, on the other hand, converts wet biomass into a liquid fuel under high pressures of 5–20 MPa and moderate temperatures in the absence of oxygen. However, it is less widely adopted for hydrogen production due to its complex operational requirements and low hydrogen selectivity.[8], [10], [16]

- Gasification

  Biomass is heated at high temperatures ranging from 500°C to 1400°C, in the presence of limited oxygen or steam. The process generates syngas (mainly H_2, CO, CO_2, CH_4), from which hydrogen is extracted after cleaning and water-gas shift (WGS) reactions. The common feedstocks used in this process include wood chips, crop residues and organic waste. Some key concerns involved with this biomass decomposition method include, ash content, moisture, and tar formation.[10], [16]

- Pyrolysis

  This is a thermochemical method that breaks down biomass into a mixture of gases, liquids and solids by heating it in the absence of oxygen, typically at temperatures between 650 and 800K and pressures of 0.1 to 0.5 MPa[8], [10]. In some designs, a small amount of oxygen is intentionally introduced to enable partial combustion, which provides the heat necessary to

sustain the process internally[17]. The process produces hydrogen, carbon monoxide, methane, tar, and charcoal, among other products. While hydrogen is formed directly, further hydrogen can be extracted by treating the resulting carbon monoxide and hydrocarbon gases using additional processes such as steam reforming and the water-gas shift reaction. The final purification of hydrogen is typically achieved using pressure swing adsorption (PSA) to meet high-purity standards. [16]

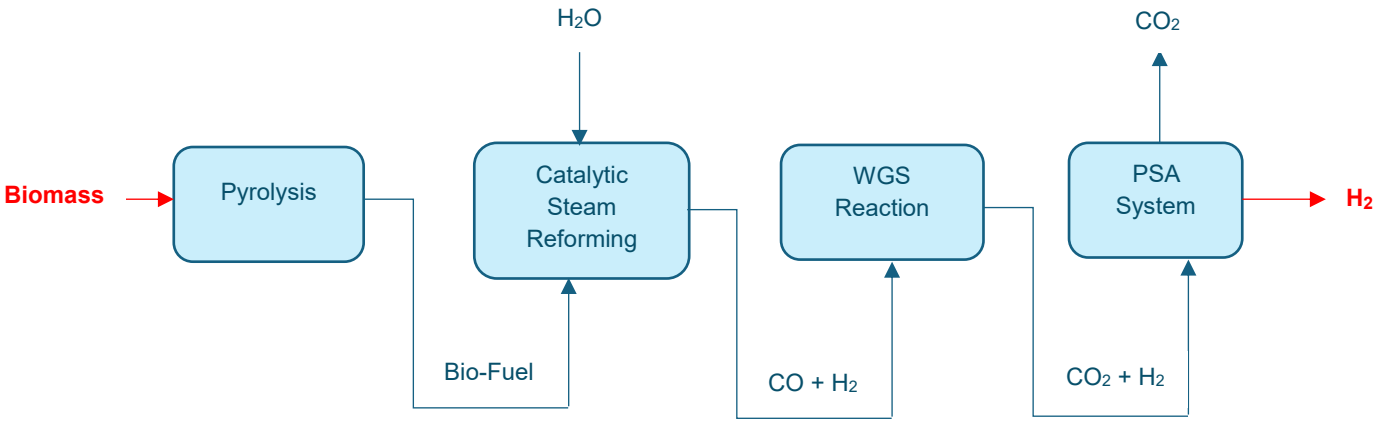

Figure 1.6: Flow diagram of the biomass pyrolysis process [8]

1.7.2.1.2. Biochemical Methods

Biochemical hydrogen production involves the use of microorganisms such as bacteria, algae, or enzymes to generate hydrogen under mild, environmentally friendly conditions. This renewable method has gained attention due to its potential in sustainable development and waste reduction. However, major obstacles include low conversion efficiency, sensitivity to oxygen, and difficulty scaling up the systems for industrial use[8], [10]. *Fermentation* and *Bio-photolysis* are the two main biological processes utilized to produce hydrogen.

- Bio-photolysis

This method is inspired by the natural photosynthesis processes in plants, algae and cyanobacteria. Using light energy, these organisms can split water molecules into hydrogen and oxygen. In **direct bio-photolysis**, green algae absorb sunlight to drive water-splitting, producing hydrogen ions and oxygen. The hydrogen ions are then converted to hydrogen gas by a highly oxygen-sensitive enzyme known as hydrogenase, requiring oxygen levels below 0.1%. [8], [10]

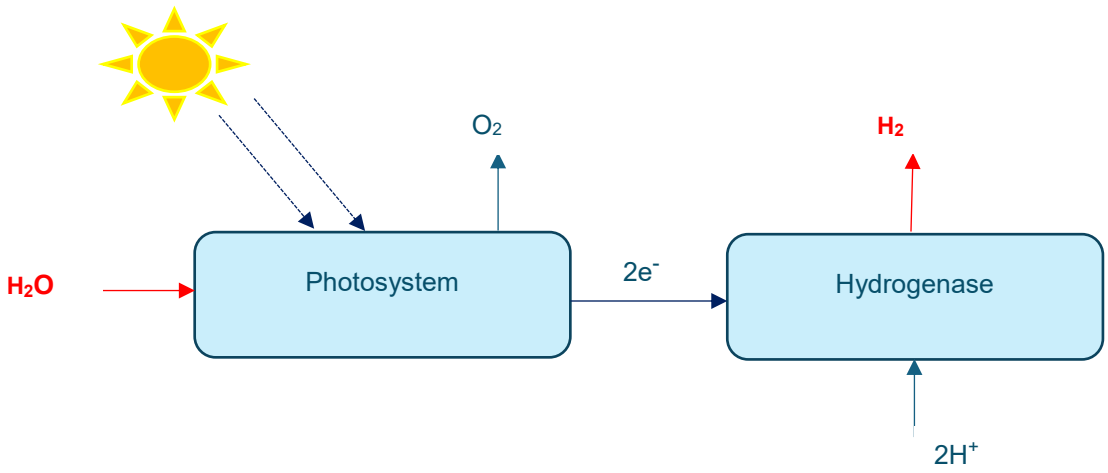

Figure 1.7: Flow diagram of the direct bio-photolysis process [8]

In **indirect bio-photolysis**, the microorganisms first produce biomass via photosynthesis. Later, the stored organic compounds are broken down to release hydrogen. This process often involves cyanobacteria (blue-green algae) and proceeds through a two-stage mechanism: biomass formation followed by hydrogen production. Bio-photolysis methods are appealing for their use of water and sunlight but are limited by the low stability of enzymes and the need for strict oxygen control.[10], [16]

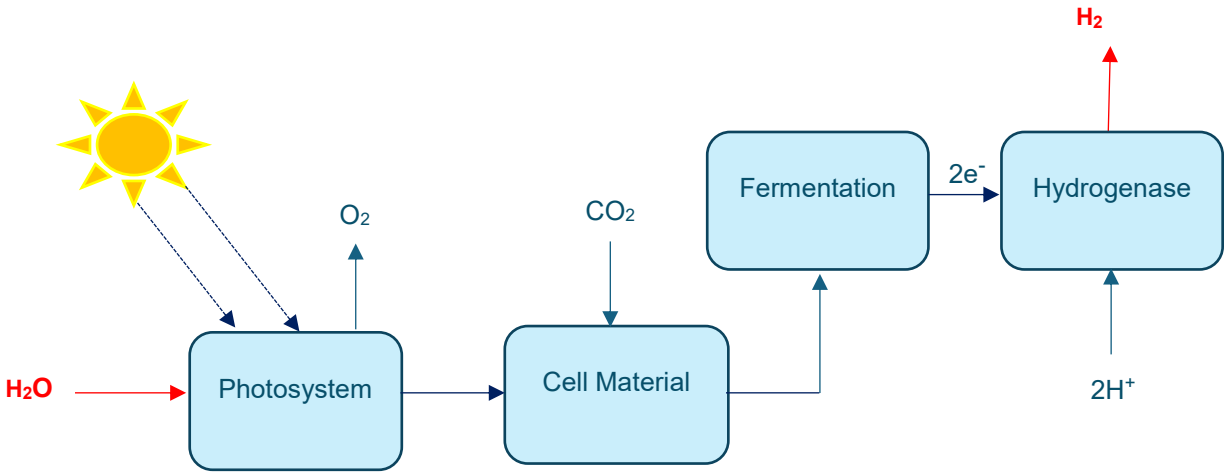

Figure 1.8: Flow diagram of the indirect bio-photolysis process [8]

- Fermentation

Fermentation processes use microbes to convert organic substrates into hydrogen under anaerobic conditions. This technique is particularly promising because it can utilize organic

waste materials as feedstock, providing both energy production and waste minimization. In **Dark Fermentation**, anaerobic bacteria break down carbohydrate-rich materials (like glucose or starch) in the absence of oxygen and light. It occurs at relatively low temperatures and produces hydrogen along with by-products like volatile fatty acids and carbon dioxide. Although the hydrogen yield is relatively low, dark fermentation is simple and can run continuously using agricultural or food waste.[10]

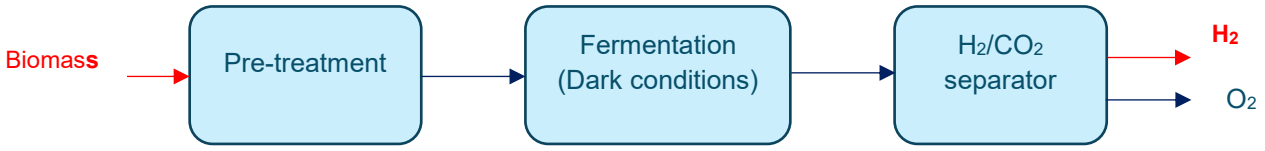

Figure 1.9: Flow diagram of the dark fermentation process [8]

Photo-fermentation involves photosynthetic bacteria that use light energy and organic acids (such as acetic or butyric acid) under nitrogen-limited conditions to produce hydrogen. The key enzyme responsible is nitrogenase, which enables the conversion of these acids into H_2 and CO_2. This method complements dark fermentation, as the by-products from the latter can be used as substrates in photo-fermentation.[16]

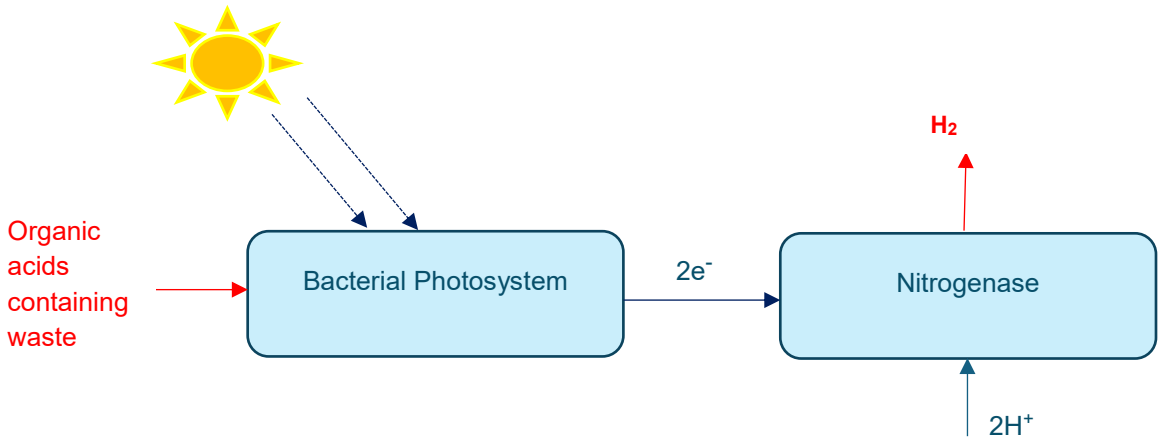

Figure 1.10: Flow diagram of the photo-fermentation process[8]

1.7.2.2. Water Splitting Methods

Water is one of the most abundant and inexhaustible raw materials on Earth and can be used for hydrogen production through water-splitting processes such as electrolysis, thermolysis and photo-electrolysis. This is the cleanest and most sustainable way to produce hydrogen, with zero carbon emissions when powered by renewable energy sources like solar and wind. Hydrogen produced this way with zero carbon emissions is termed “Green Hydrogen”. [18]

1.7.2.2.1. Thermolysis

Thermolysis is the process by which water is heated to a high temperature over 2500°C until decomposed to hydrogen and oxygen. The source of heat could be nuclear reactor or solar concentrators. The decomposition is shown in the equation below:

$2H_2O \rightarrow 2H_2 + O_2$; $T > 2500°C$ [8]

Since this process of Thermolysis is energy intensive, requiring extremely high temperatures, an alternative can be used, that is, *Thermochemical Water Splitting,* this process uses a series of chemical reactions at lower temperatures (500–1000°C) to split water indirectly. An example of this process is the Copper-Chlorine (Cu-Cl) Cycle: [8]

Step 1: Hydrolysis (Cu_2OCl_2 Formation)

$2CuCl_2(s) + H_2O(g) \rightarrow Cu_2OCl_2(s) + 2HCl(g)$ $T=400^oC$

Step 2: Oxygen Evolution

$Cu_2OCl_2(s) \rightarrow 2CuCl(l) + \frac{1}{2}O_2(g)$ $T=500^oC$

Step 3: Dissolution reaction

$4CuCl(s) + H_2O(l) \rightarrow 2CuCl_2(aq) + 2Cu(s)$ $T=25\text{-}80^oC$

Step 4: Drying

$CuCl_2(aq) \rightarrow CuCl_2(g)$ $T=100^oC$

Step 5: Hydrogen Evolution

$2Cu(s) + 2HCl(g) \rightarrow 2CuCl(l) + H_2(g)$ $T=430\text{-}475^oC$

1.7.2.2.2. Electrolysis

- Basic Principle:

Electrolysis is an electrochemical process that splits water into hydrogen and oxygen using electrical energy. It is governed by the following half-reactions:

Anode (Oxidation): $2H_2O \rightarrow O_2 + 4H^+ + 4e^-$

Cathode (Reduction): $4H^+ + 4e^- \rightarrow 2H_2$

Overall Reaction: $2H_2O \rightarrow 2H_2 + O_2$

The minimum theoretical voltage required is 1.23V under standard conditions. However, real-world operation requires a higher voltage due to system inefficiencies.[19]

➢ Types of Electrolyzers

Several technologies enable water electrolysis, each with distinct operating conditions, maturity levels, and suitability for renewable integration:

Type	Electrolyte	Temperature range	Advantages	Limitations
Alkaline	KOH/NaOH (Liquid)	70-90°C	Low cost, mature, simple design	Bulky, lower purity, slower response
PEM(Proton Exchange Membrane)	Solid Polymer	50-80°C	High purity, compact, fast response	Expensive, sensitive to water quality
SOEC(Solid Oxide Electrolysis Cell)	Ceramic Oxide	700-1000°C	High efficiency, uses waste heat	Expensive, still in development

Table 1.4: Summary of the three types of electrolysers[20]–[22]

Chapter 2 will explore these in detail, focusing on their technical performance and compatibility with solar PV systems.

➢ Key Efficiency Concepts

Electrolysis performance depends on several critical factors:

1) Overpotentials: Extra voltage beyond 1.23V required to drive the reactions, due to:
   - Activation losses: Related to electrode kinetics.
   - Ohmic losses: Resistance in the electrolyte/membrane.
   - Concentration losses: Due to mass transport limitations.[18]
2) Faradaic Efficiency: Ratio of actual hydrogen produced to theoretical maximum, accounting for side reactions or gas losses.[23]

These parameters are particularly important when coupling electrolysis to variable power sources like solar.

➢ Energy Sources for Electrolysis

Electrolyzers can be powered from a variety of energy sources, each influencing the carbon footprint of hydrogen:

- Grid Electricity:

Widely used but often carbon-intensive unless the grid is renewable-powered.

Example: Alkaline electrolyzers drawing from fossil-fuel-dominated grids.[10]

- Renewable Energy:

Hydrogen production via electrolysis can be driven by various renewable sources, each offering specific benefits and challenges:

1. Wind Power: Offers a higher capacity factor than solar, but typically requires large installations and may be less suited for modular or decentralized hydrogen production.
2. Hydropower: Provides a stable and dispatchable electricity source, but is limited by geographical and environmental constraints.
3. Biomass: Can produce hydrogen through gasification, but its scalability is constrained by feedstock availability and logistics.
4. Geothermal: Offers continuous power but is limited to specific regions with accessible geothermal resources.[10], [16]

Despite the diversity of options, solar photovoltaic (PV) energy stands out as a particularly attractive candidate for green hydrogen production, especially in regions with high solar irradiance.

- Why Solar PV is Ideal for Electrolysis

Solar PV has several key characteristics that make it highly compatible with electrolysis systems:

- Abundant and Ubiquitous: Solar energy is available in most parts of the world, with exceptional potential in sun-rich areas such as Algeria and other parts of Africa.
- Declining Costs: The cost of solar PV modules has dropped significantly in the past decade, making solar-powered hydrogen production increasingly competitive.
- Modularity and Scalability: PV systems can be deployed at various scales, from small off-grid setups to utility-scale plants, allowing flexible integration with different electrolyzer sizes.
- Synergy with PEM Electrolyzers: Proton Exchange Membrane (PEM) electrolyzers are well-suited for coupling with solar PV due to their fast response time and ability to operate under dynamic input conditions.
- Environmental Benefits: Unlike fossil-based power, solar PV does not emit greenhouse gases during operation, enhancing the sustainability of the overall hydrogen production process.[10]

This thesis will therefore focus on PV-powered electrolysis due to its relevance for sustainable hydrogen production in Algeria. The integration of solar systems with electrolyzers, perfomance challenges and optimization approaches are explored in detail in Chapter 2.

1.7.3. Colour-Coded Classification of Hydrogen Production

Hydrogen is often classified by a color-coded spectrum that indicates the source and carbon footprint of its production. This informal system, while not technically standardized, is widely used in policy and industry discourse. The main categories include:

- Grey Hydrogen: Produced from natural gas via steam methane reforming (SMR) without carbon capture. It is currently the most common but emits around 9–12 kg of CO_2 per kg of H_2.

- Blue Hydrogen: Also from SMR or coal gasification, but with carbon capture and storage (CCS) systems to reduce emissions. Its climate benefit depends heavily on the capture rate and lifecycle emissions of the CCS infrastructure.

- Green Hydrogen: Produced through electrolysis powered by renewable energy sources (solar, wind, hydro). It is considered the cleanest form, with near-zero direct emissions.

- Turquoise Hydrogen: Derived from methane pyrolysis, producing solid carbon instead of CO_2. It is still in early development, and its sustainability hinges on energy inputs and carbon handling.
- Pink Hydrogen: Generated via electrolysis powered by nuclear energy. While it avoids CO_2 emissions, it raises questions about nuclear safety and waste.
- Brown/Black Hydrogen: Obtained from coal or lignite gasification without CCS. It has the highest emissions and is the least sustainable option.

Type	Production method	CO_2 Impact	Cost (2023) [€/kg]
Grey	Steam Methane Reforming (SMR)	High	€1.5-2.0
Blue	SMR + Carbon Capture (CCS)	Medium	€2.0-3.5
Green	Electrolysis (Solar/Wind)	Low	€4.0-8.0
Turquoise	Methane Pyrolysis	Low(Solid carbon by-product)	€ 2.5-4.5
Pink	Electrolysis(nuclear power)	Low	€ 3.0-5.0
Brown/Black	Coal gasification	Very high	€ 1.2-2.0

Table 1.5: Classification of hydrogen production methods based on color [10], [20]

1.8. Hydrogen Storage and Transportation

Once produced, hydrogen must be stored and transported safely and efficiently to meet the demands of various end-use applications. Unlike conventional fuels, hydrogen has a low volumetric energy density in its gaseous form, which presents technical and economic challenges for storage and distribution. As a result, several storage methods have been developed, each with its own trade-offs in terms of cost, complexity, energy requirements and safety.

1.8.1. Storage

There are various ways to store hydrogen: in pressure vessels, as liquid hydrogen, as metal hydrides and in underground storages. For large volumes, the techniques used are those of liquid hydrogen and underground storage. Hydrogen storage methods can generally be classified into two broad categories based on the underlying storage mechanism: physical-based and material-based storage. [10], [24]

1.8.1.1. Physical-based storage

Involves retaining hydrogen in its molecular form, either as compressed gas, liquid hydrogen, or cryo-compressed hydrogen, relying on pressure and temperature conditions to increase energy density. These methods are technologically mature and commonly used in industry but require high energy input for compression or liquefaction and present safety challenges. The storage of liquid hydrogen at a temperature of -253°C is practiced on an industrial scale using vacuum-insulated spherical tanks. The largest storage facilities are those set up on rocket launch sites.[24]

1.8.1.2. Material-based storage

Involves storing hydrogen by interaction with solid or liquid materials. This includes chemical sorption, where hydrogen forms reversible chemical bonds with substances such as metal hydrides, ammonia, and liquid organic hydrogen carriers (LOHCs), and physical sorption, where hydrogen is adsorbed onto high-surface-area materials like activated carbon, zeolites, metal-organic frameworks (MOFs), and glass microspheres. Material-based storage methods offer promising advantages in terms of volumetric density and safety but are still largely in the development phase due to limitations in kinetics, operating conditions, and cost. This classification provides a more mechanistic understanding of hydrogen storage options and is widely used in research and advanced energy system design. [2], [10]

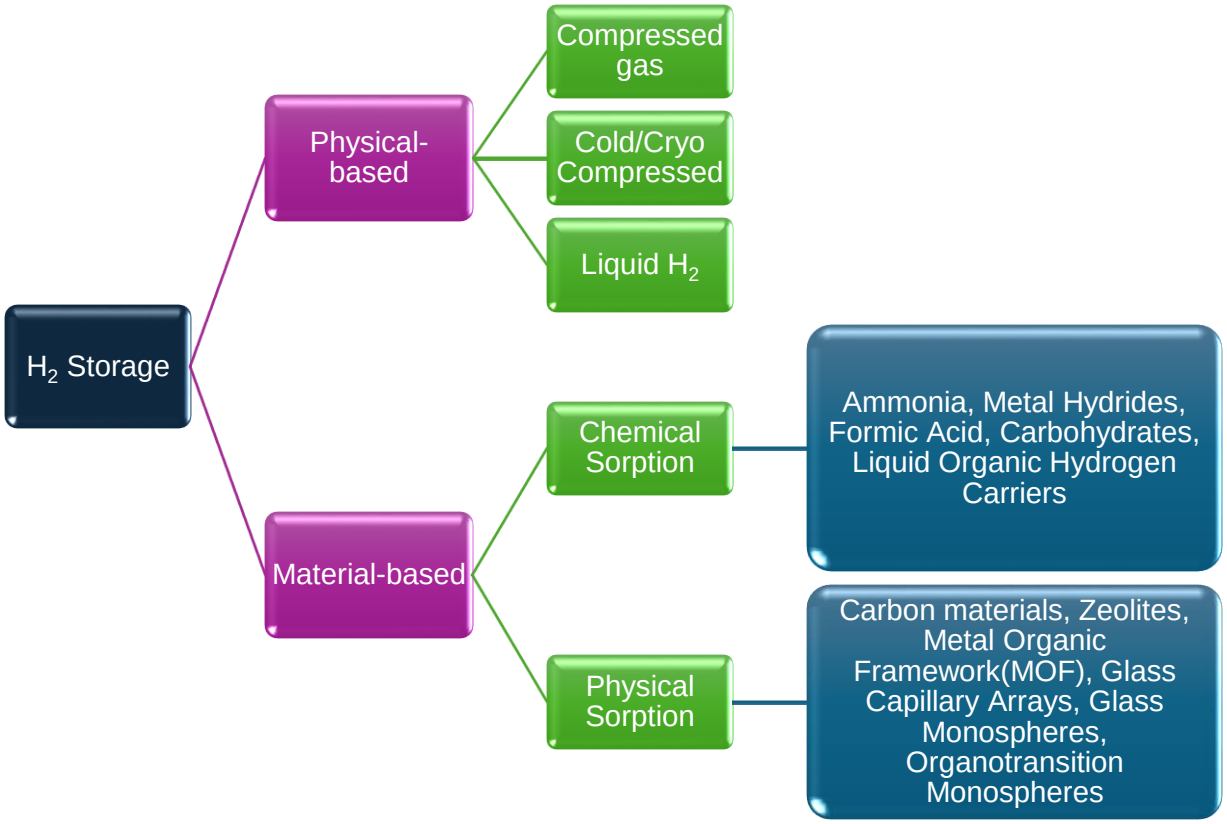

Figure 1.11: Hydrogen storage methods[2], [10], [24]

1.8.2. Transportation

Transporting hydrogen from production sites to end users is a critical component of the hydrogen value chain, particularly as demand scales across sectors and regions. Due to hydrogen's low volumetric energy density, specialized infrastructure and strategies are required to ensure efficiency, safety and economic viability.

1.8.2.1. Gaseous Hydrogen Transportation

Hydrogen is most commonly transported in gaseous form through high-pressure pipelines or in compressed gas cylinders.

Pipelines: Suitable for large-scale, continuous transport over short to medium distances. Existing natural gas pipelines can be repurposed or blended with hydrogen (typically up to 20%) with minimal modifications, though pure hydrogen pipelines require specific materials to avoid embrittlement.

Tube Trailers: For road transport, hydrogen is stored at pressures of 200–700 bar in high-strength steel or composite cylinders mounted on trailers. This method is flexible but limited by volume and pressure regulations.[2]

1.8.2.2. Liquid Hydrogen Transportation

Hydrogen can be liquefied at cryogenic temperatures (~−253°C), reducing volume and enabling bulk transport.

Cryogenic Trucks: Liquid hydrogen is transported in insulated tanks over long distances. It offers higher volumetric density than gas but incurs high energy losses (about 30% of the energy content) during liquefaction.

Maritime Shipping: In global hydrogen trade scenarios, liquid hydrogen tankers may enable intercontinental transport, though this is still in early development stages.[2], [10]

1.8.2.3. Hydrogen Carriers (Material-Based Transport)

To overcome storage and transport limitations of pure hydrogen, hydrogen carriers offer promising alternatives. These include:

Ammonia (NH_3): Easily liquefied, has high hydrogen density, and existing infrastructure. Hydrogen is recovered via cracking (decomposition) at the point of use.

Liquid Organic Hydrogen Carriers (LOHCs): Organic compounds (e.g., dibenzyltoluene) that absorb and release hydrogen through catalytic processes. They are non-toxic and can be handled like conventional fuels.

Metal Hydrides: Solid compounds that store hydrogen by forming metal-hydrogen bonds. Offer high density but are typically heavy and slow in release.

These carriers allow hydrogen to be transported using existing fuel infrastructure (tanker trucks, ships) and are particularly useful in regions without pipeline access.[24]

1.9. Conclusion

Hydrogen emerges as a pivotal element in the global energy transition due to its versatility, high energy density, and potential for decarbonization[2]. This chapter explored its fundamental properties, historical significance, and diverse applications, from industrial feedstock to fuel. The analysis highlighted key production methods, including steam reforming, pyrolysis, and electrolysis, with a clear distinction between non-renewable (grey/blue hydrogen) and renewable (green hydrogen) pathways. Storage and transportation remain critical challenges, with solutions ranging from compressed gas and cryogenic liquid hydrogen to material-based carriers (e.g., ammonia, LOHCs). While hydrogen offers advantages like zero-emission combustion, hurdles such as infrastructure costs, energy-intensive production, and safety concerns must be addressed. The chapter underscores hydrogen's strategic role in decarbonizing hard-to-abate sectors (e.g., steel, aviation) and sets the stage for exploring sustainable production methods, particularly solar-integrated electrolysis, in subsequent chapters.

2 Chapter 2: Electrolysis and Solar Integration for Green Hydrogen

2.1. Introduction

Hydrogen production through water electrolysis has emerged as a cornerstone technology in the transition to cleaner energy systems, especially when powered by renewable sources[16]. Among the various green hydrogen strategies, solar-powered electrolysis is particularly attractive due to its sustainability and scalability. This chapter explores the main solar-driven electrolysis pathways, photo-electrochemical (PEC), photocatalytic, and PV-powered electrolysis, highlighting their principles, challenges and development status. Following this comparison, the focus shifts to PV-powered electrolysis, the most mature and commercially viable approach, which serves as the foundation for the simulation work in this study.

2.2. Electrolysis Principles

2.2.1. Fundamental Reactions

Water electrolysis occurs in an electrolyser which consists of two electrodes (anode and cathode) submerged in an electrolyte (aqueous or solid) and separated by a membrane. By the use of electrical energy, H_2O is split into H_2 and O_2 via two half-reactions occurring at the electrodes: [19]

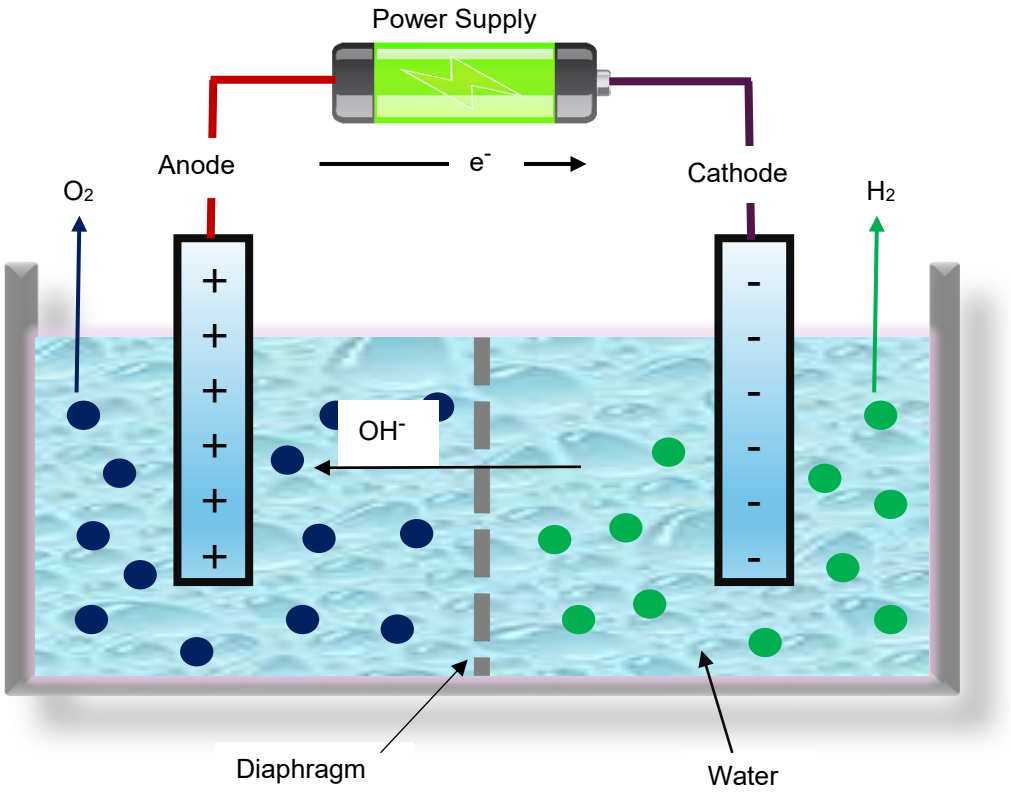

Figure 2.1: General setup of water electrolysis

- In Acidic Media (PEM Electrolysers):

Anode (Oxidation): $2H_2O \rightarrow O_2 + 4H^+ + 4e^-$

Cathode (Reduction): $4H^+ + 4e^- \rightarrow 2H_2$

- In Alkaline Media (Alkaline Electrolysers):

Anode: $4OH^- \rightarrow O_2 + 2H_2O + 4e^-$

Cathode: $4H_2O + 4e^- \rightarrow 4OH^- + 2H_2$

- Overall Reaction (Both Cases):

$2H_2O \rightarrow 2H_2 + O_2$ [25]

2.2.2. Thermodynamics and Voltage Requirements

The energy demand for water splitting is defined by thermodynamics:

2.2.2.1. Reversible Voltage (E_{rev}):

The minimum voltage required under standard conditions (25°C, 1atm) is derived from Gibbs free energy, ΔG = 237.2 kJ/mol:

$$E_{rev} = \frac{\Delta G}{nF} = 1.23V$$

Where: n = 2; number of electrons per H_2 molecule

F = 96 485 C/mol; Faraday's constant

However, practical systems require higher voltage due to irreversible losses including overpotentials (activation, ohmic, concentration) and system inefficiencies. We then talk of the cell operating voltage $E_{cell,}$ which is between 1.8 and 2.2V in real electrolysers. [23]

2.2.2.2. Temperature Effects on E_{rev}:

The thermodynamic voltage requirement is temperature-dependent. As temperature increases, the Gibbs free energy decreases, leading to a lower theoretical voltage. This dependence is captured in an empirical relation for the temperature-corrected reversible voltage $E_{rev}(T)$:

$$E_{rev}(T) = 1.5184 - 1.5421 * 10^{-3}T + 9.523 * 10^{-5}\,\mathrm{Tln}(T) + 9.84 * 10^{-8}\,T^2$$

Where T is the absolute temperature in Kelvin. This formulation reflects the thermodynamic minimum voltage under varying thermal conditions, which is particularly relevant in solar-powered systems subjected to daily and seasonal temperature variations.

The total voltage is therefore:

$E_{cell} = E_{rev}(T) + \eta_{total}$; η_{total} is the sum of all the overpotentials.[26]

2.2.2.3. Electrolyte Conductivity and Temperature:

Electrolyte performance also varies with temperature. As temperature rises, ionic conductivity improves, which reduces ohmic losses. This effect is modelled using a temperature coefficient:

$$K(T) = K_{25}[1 + \alpha(T - 25)]$$

Where:

K_{25} is the conductivity at 25 °C

α is the temperature coefficient (typically 0.02–0.06 $°C^{-1}$)

T is the ambient temperature in °C [26]

These equations form the thermodynamic and electrochemical basis of the voltage and efficiency calculations used in the simulation model.

2.3. Electrolyser Technologies

2.3.1. Alkaline Electrolyser

The alkaline electrolyser is the most widely used technology for water electrolysis. It uses a liquid alkaline electrolyte with a pH greater than 7 (KOH or NaOH), the concentration of electrolyte must be high enough to ensure good mobility of the ions, typically potassium hydroxide concentrations of 30% or more are required. Typical electrode materials for cathodes in alkaline electrolysers are Ni, Fe, Co, Zn, Pb, Pd, Pt, and Au; while Ni, Pt, Ir, Ru, Rh, titanium dioxide, and Co are used for the anodes. Suitable electrodes for AWE electrolysers, should have material with high corrosion resistance, high conductivity, high surface area and high catalytic effect and must have a long life such as nickel-based metals. The electrodes are separated by a porous solid material (diaphragm) that allows the transport of OH^- ions between the electrodes. The diaphragm exhibits a very low permeability to oxygen and hydrogen, it separates the produced gases and prevents mix-ups that could lead to safety hazards and low faradaic efficiencies. Commercial alkaline electrolysers have efficiencies in the range of 60–75%, while advanced systems currently under development can exceed 90%, operates at 70–90°C. An alkaline electrolyser for hydrogen production requires a comprehensive water treatment plant. The purity of water can be a major concern in water electrolysis. The presence of metal atoms in the water, such as calcium or magnesium, can cause reactions on the electrode surface that eventually lead to the formation of mineral deposits, which reduces the active surface area and enhances the blockage of the diaphragm. The salinity of the water is also important, if the water contains sodium chloride or chloride ions from other sources, the chlorine will have a highly corrosive effect at the cathode. Typically, commercial alkaline electrolysers operate at current densities between 1 and 6 kAm^{-2}, while advanced alkaline electrolysers operate at densities of 2–15 kA m^{-2}. [21], [23], [27]

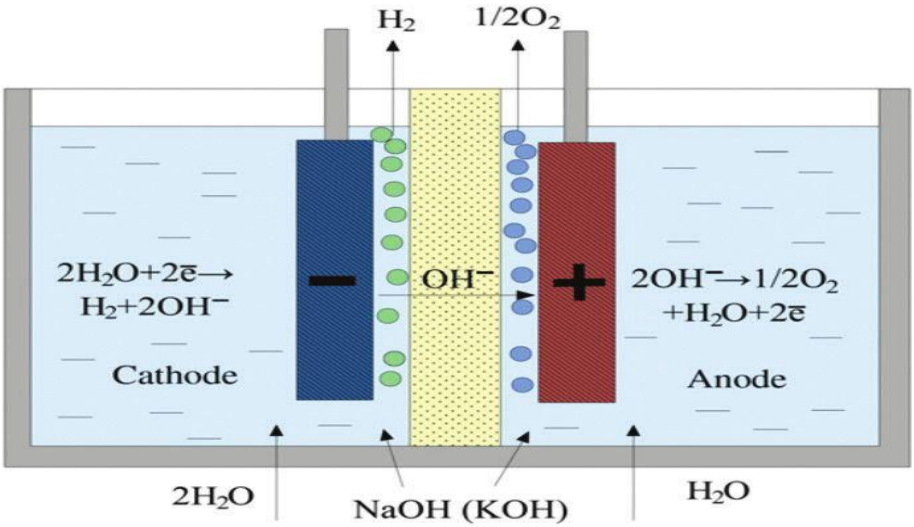

Figure 2.2: AEL Cell[28]

Anode: $4OH^- \rightarrow O_2 + 2H_2O + 4e^-$

Cathode: $4H_2O + 4e^- \rightarrow 4OH^- + 2H_2$

2.3.2. Proton Exchange Membrane (PEM) Electrolyser

In PEM cells, there is no liquid electrolyte, only deionized water circulates. The central component of the cell is a thin (≈0.2mm thick) membrane of a proton-conduction polymer electrolyte. Such cells are very compact and the efficiency of water splitting is high. The membrane is used for the double purpose of carrying ionic charges (solvated protons) and separating electrolysis products (molecular hydrogen and oxygen), thus preventing their spontaneous exothermic recombination into water. On both side of the membrane, two porous catalytic layers are coated, these catalytic layers are connected to an external DC power source that provides electrical work for the electrolysis reaction. The PEM operates at 50–80°C, offering higher efficiency and faster response times but is still considered as an expensive technology due to the use of noble metal catalysts (e.g., Pt, Ir). In these cells, DC current is used to split liquid water into gaseous oxygen and protons at the anode. In response to the electrical field set across the cell, solvated protons migrate down to the cathode where they are desolvated andreduced into molecular hydrogen. Carbon-supported platinum nanoparticles are used as the electrocatalyst at the cathode for the promotion of HER. At the anode, Iridium (metal or oxide) is the most efficient and stable catalyst for the OER in acidic media.[20]

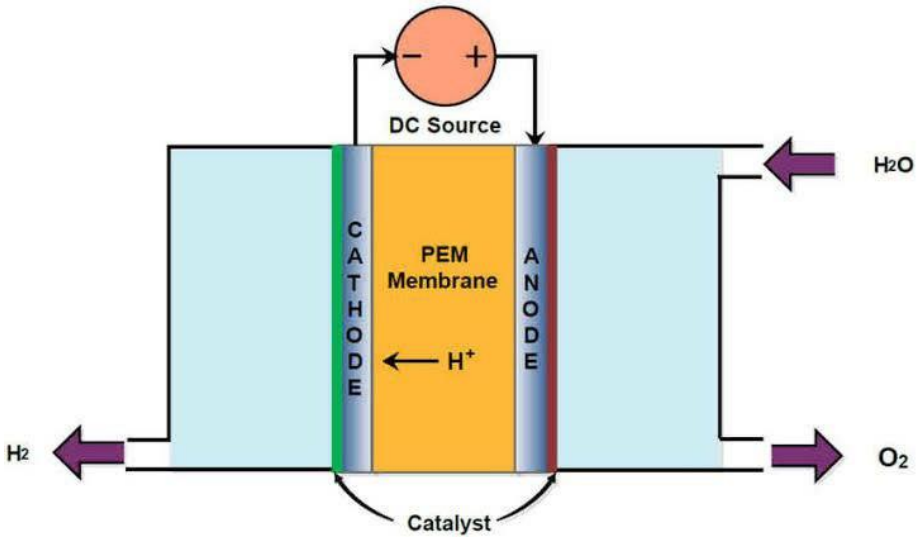

Figure 2.3: PEM Electrolyser

Anode: $2H_2O \rightarrow O_2 + 4H^+ + 4e^-$

Cathode: $4H^+ + 4e^- \rightarrow 2H_2$

2.3.3. Solid Oxide Electrolysis (SOEC)

Operates at high temperatures (700–1000°C)[21], using a ceramic electrolyte that selectively conducts negatively charged oxygen ions (O^{2-}). As the splitting of water is an endothermic reaction, electricity demand and decomposition voltage decrease with an increase in temperature. Therefore it is beneficial to operate at elevated temperatures for water electrolysis. Overpotentials and ohmic voltage drops decrease considerably at high operation temperatures. High-temperature SOECs are reversibly operated solid oxide fuel cells (SOFCs). SOFC is an energy conversion device to electrochemically convert chemical energy of fuels such as hydrogen, hydrocarbons, and biofuels to electricity. More efficient due to reduced energy input and no expensive electrocatalysts are required due to the high operating temperatures but compared with commercial alkaline electrolyzers and PEM electrolyzers, the SOECs are still in the early stage of development. However, it is a promising technology for large-scale hydrogen production and attracts wide research interests.[16]

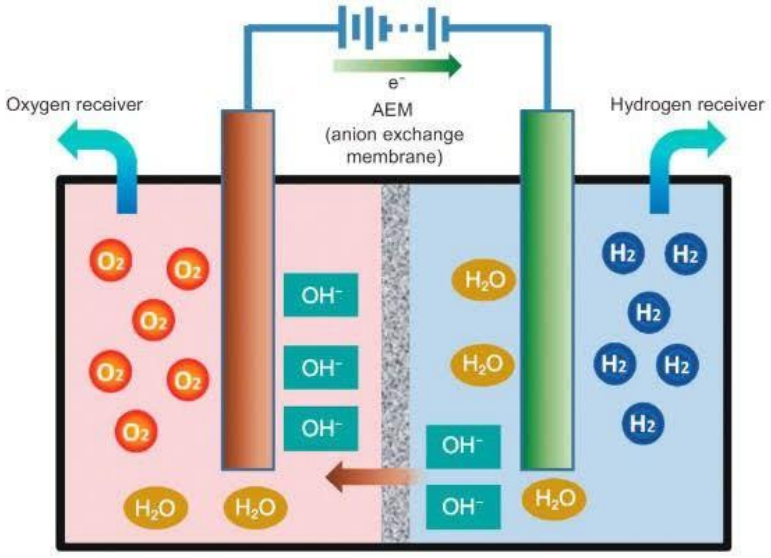

Figure 2.4: SOEC[29]

Anode: $4OH^- \rightarrow O_2 + 2H_2O + 4e^-$

Cathode: $2H_2O + 2e^- \rightarrow 2OH^- + H_2$

2.3.4. Comparative Analysis

Parameter	AEL	PEMWE	SOEC
Efficiency (LHV)	60-75%	65-82%	85-95%
Capital Cost (€/kW)	450-950€	1200-1800€	1800-3200€
Current Density	0.2-0.5 A/cm^2	1-3 A/cm^2	0.5-1.5 A/cm^2
Response Time	Minutes	Seconds	Hours
Solar Compatibility	Slow response	Excellent (fast)	Fair (Requires heat)
Lifespan (years)	7-11	4.5-7	1-2.5

Table 2.1: Comparative analysis of electrolysers[10], [20], [21]

2.4. Efficiency and Losses in Electrolysis

Electrolysis performance is governed by a range of physical and electrochemical factors that introduce energy losses and influence the overall system efficiency. These losses are essential when evaluating and designing solar-powered electrolysis systems, because they directly affect hydrogen yield, system sizing and cost. This section outlines the main contributors to electrolysis inefficiency: Overpotentials, Faradaic efficiency and energy efficiency metrics.

2.4.1. Faradaic Efficiency

In general, efficiency is defined as the ratio of useful output to total input. For electrolysis, Faradaic efficiency specifically quantifies how effectively the input electrical charge is converted into chemical energy stored in hydrogen. It is commonly expressed as the ratio of the actual hydrogen production rate to the theoretical rate derived from the applied current:[23]

$$\eta_F = \frac{\dot{n}_{H2\ actual}}{\dot{n}_{H2\ theoretical}}$$

The theoretical hydrogen production rate, assuming 100% efficiency, is derived from the Faraday's law:

$$n_{H2\ theoretical} = \frac{Q}{z.F} = \frac{I.t}{z.F}$$

Dividing both sides by time 't':

$$\dot{n}_{H2\ theoretical} = \frac{I}{z.F}$$

In practice, not all current contributes to hydrogen evolution due to losses (e.g. side reactions, recombination), the actual hydrogen flow rate becomes:

$$\dot{n}_{H2\ actual} = \eta_F * \dot{n}_{H2\ theoretical} = \eta_F * \frac{I}{z.F} = \eta_F * \frac{P}{z.F.V}$$

In the simulation in Chapter 3, current is not directly stated but is instead expressed through the applied electrical power 'P' and cell voltage 'V' using the relation; $I = \frac{P}{v}$

We then end up having:

$$\dot{n}_{H2\ theoretical} = \eta_F * \frac{P}{z.F.V}$$

Typical Faradaic efficiencies are close to 100% in well-designed systems but can drop due to membrane leakage, side reactions, or poor operating conditions.

system-level efficiencies range from 60–70%, depending on technology, current density, and operating conditions.

2.4.2. **Overpotentials**

Overpotentials represent the extra voltage required beyond the theoretical minimum (reversible voltage) to drive the electrolysis reaction at a practical rate. They arise due to resistances and kinetic barriers at the electrodes and within the electrolyte. The overpotentials involved in voltage loss in electrochemical processes include activation (η_{act}), ohmic (η_{ohm}), and concentration (η_{conc}) overpotentials. They can be expressed as follows:

$$\eta_{total} = \eta_{act} + \eta_{ohm} + \eta_{conc}\ [22]$$

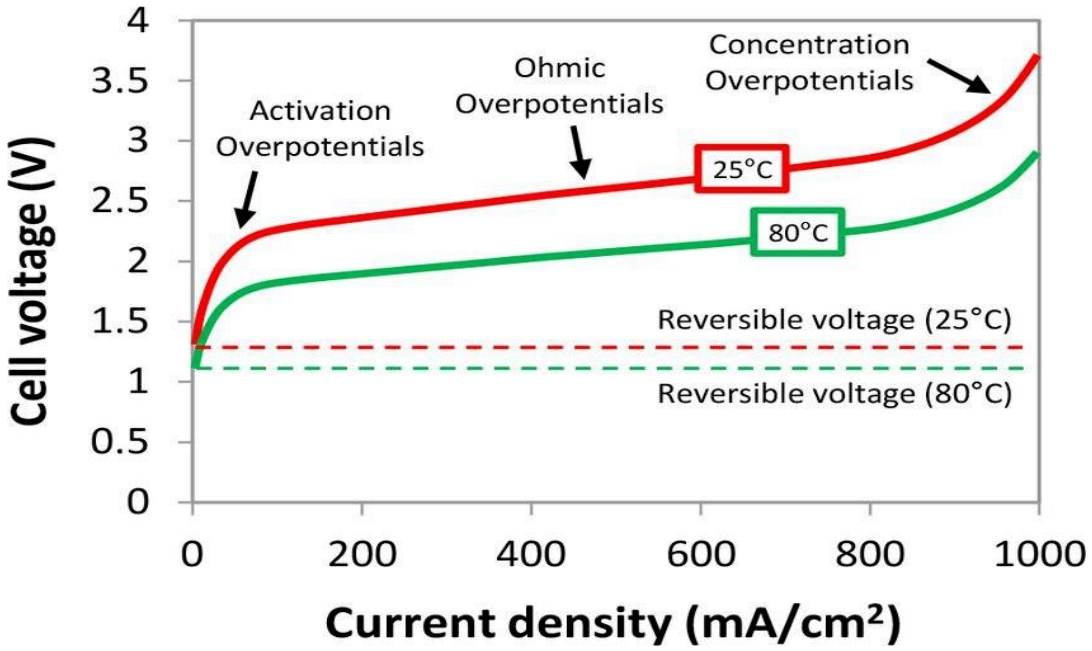

Figure 2.5: Reversible voltage and overpotentials[22]

2.4.2.1. Activation Overpotential (ηact) and the Butler–Volmer Equation

The activation overpotential reflects the kinetic loss of electrochemical reactions that take place at the electrode surface during the water electrolysis process that correlate to the activation energy of these reactions. In other words, activation overpotential arises due to the energy barrier that must be overcome for electrochemical reactions to occur at the electrode–electrolyte interface. It is particularly significant in water electrolysis, where the oxygen evolution reaction (OER) at the anode and the hydrogen evolution reaction (HER) at the cathode both exhibit sluggish kinetics that limit overall efficiency.[18], [23]

The kinetics of charge transfer reactions are commonly described using the Butler–Volmer equation, which relates the current density (J) to the activation overpotential (η_{act}) as follows:[30]

$$J = J_0 \left[exp\left(\frac{\alpha F \eta}{RT}\right) - exp\left(-\frac{(1-\alpha) F \eta}{RT}\right)\right]$$

Where:

J = current density [A/m²]

J_0= exchange current density [A/m²]

α= charge transfer coefficient (0.2–0.5)

η= activation overpotential [V]

This nonlinear equation cannot be directly inverted to isolate η; therefore, numerical methods such as the Newton-Raphson iterative technique are used to compute the activation overpotential for a given set of parameters. The method starts from an initial estimate and iteratively refines the value using the derivative of the Butler–Volmer expression until convergence is achieved. In practice, activation overpotentials are calculated separately for each electrode:

Anode (OER): Using parameters like the anode's exchange current density ($J_{0,anode}$), charge transfer coefficient (α_{anode}), and temperature .

Cathode (HER): Similarly, parameters like $J_{0,cathode}$ and $\alpha_{cathode}$ govern the HER kinetics.

The total activation overpotential is the sum of both contributions from the two electrodes:

$$\eta_{act,total} = \eta_{act,anode} + \eta_{act,cathode}$$

These overpotentials increase with current density and dominate at high current operation, impacting system voltage and efficiency.

2.4.2.2. Ohmic Overpotential (η_{ohm}):

Ohmic overpotentials generally result from the electrical resistance of the electrolyte, electrodes, and membrane. They originate from two aspects: the ion conducting resistance (relates to the ion component flow through the electrolyte) and the electronic resistance (represents the electronic component flow through the external circuit). In AWE electrochemical system, the ohmic overpotential is mainly contributed by the ion conducting resistance, because the electronic resistance accounts for a very low percentage of overall ohmic loss. Since a liquid is used as the electrolyte in AWE, the effect of bubbles in the electrolyte on the ion transport is more significant than that of PEMWE which uses a solid as electrolyte that can eliminate the ion transport blockage effect. Ohmic overpotential increases linearly with current:[18]

$$\eta_o = i * R_{cell} = i * \frac{d}{\sigma}$$

Where: R_{cell} includes ionic and electronic resistances; d is the electrode gap and σ is the electrolyte conductivity.

2.4.2.3. Concentration Overpotential (η_{conc}):

The concentration overpotential depends on the concentration gradients of reactants, intermediates and products. The increase in voltage need is caused by mass transport limitations, the build-up or depletion of reactants/products near the electrode surfaces, especially at high current densities when reactants can't diffuse quickly enough. This overpotential occurs when the supply of reactants such as water or hydroxide ions to the electrode or the removal of products like hydrogen

and oxygen becomes insufficient causing a concentration gradient near the electrode surface that hinders the reaction rate. The general Nernst expression is: [18]

$$\eta c = \frac{RT}{nF} ln \frac{C_b}{C_s}$$

Where: C_b = bulk concentration of the reacting species

C_s = surface concentration of the reacting species

C_s decreases with increasing current density due to diffusion limits, current is therefore linked to surface concentration:

At steady-state mass transport:

$$i = nFD.\frac{C_b - C_s}{\delta} \rightarrow C_s = C_b - \frac{i\delta}{nFD};$$

δ and D are diffusion layer thickness and diffusion coefficient respectively

The limiting current density can be defined as:

$$i_{lim} = nFD.\frac{C_b}{\delta}$$

This occurs when $C_s = 0$, so:

$$\frac{i}{i_{lim}} = \frac{C_b - C_s}{C_b} \rightarrow \frac{Cs}{C_b} = 1 - \frac{i}{i_{lim}}$$

Substituting back into Nernst form:

$$\eta c = \frac{RT}{nF} ln \frac{C_b}{C_s} = \frac{RT}{nF} ln \frac{1}{1 - \frac{i}{i_{lim}}} = \frac{RT}{nF} ln \frac{i_{lim}}{i_{lim} - i}$$

The final expression used in this study to calculate concentration overpotential is:

$$\eta c = \frac{RT}{nF} ln \frac{i_{lim}}{i_{lim} - i}$$

2.4.2.4. Bubble Effect on Overpotentials

Since water electrolysis involves the gas-evolving electrodes, gas bubbles (O_2 and H_2) will be generated on the electrode surfaces. The bubble generation and attachment on the electrodes will affect the polarization loss during the electrolysis process, which in turn affects the total overpotential losses and thus decreases the efficiency of water electrolysis and even its lifetime. Electrolysis efficiency is decreased by the presence of bubbles adhering to the electrode surfaces because they block electrode-electrolyte interface, reducing the electrode surface area available for the electrochemical reaction to take place thus increasing activation overpotential. In the liquid electrolyte of AWE both bubbles attached on the electrode and bubbles flowing in the electrolyte occupy volume, hindering the ion transport by reducing the number of available pathways for ions

to migrate (an increase in the resistance to ion transport), thus lowering the effective conductivity of the electrolyte and resulting in ohmic losses. The magnitude of the bubble-induced overpotential depends on factors such as current density, electrolyte flow rate, and electrode surface properties. To address bubble overpotentials, some recent researches are focusing on enhancing bubble separation through external methods like applying external fields, flow operation and adding surfactants to the electrolyte. Another solution is to optimize electrode wettability and structure (superhydrophilic and superaerophobic electrodes) to facilitate bubble detachment.[18]

2.5. Parameters Influencing Electrolyser Performance

The performance of an electrolyser is governed by multiple interrelated parameters that affect efficiency, hydrogen yield, and required energy input. In simulation frameworks such as the one developed in this work, certain parameters were varied to evaluate their impact on output hydrogen production and cost. Below, each key parameter is discussed in terms of its electrochemical significance and influence on performance.

2.5.1. Faradaic Efficiency (η_F)

It accounts for losses due to inefficiencies in the charge transfer process; undesirable side reactions, electrode degradation and gas crossover losses that reduce usable hydrogen output. Enhancing η_F through better catalysts, minimized gas crossover, or cell design results in a direct increase in hydrogen output per unit of electrical power.

2.5.2. Electrolyte Conductivity (σ)

Electrolyte conductivity defines the ease with which ions move between the electrodes. Low conductivity increases the internal resistance ‘R’, raising the ohmic overpotential (greater voltage losses). This in turn, increases the voltage required for electrolysis, reducing system efficiency and increasing overall energy demand. The ohmic overpotential is directly related to conductivity via:

$$\eta o = \frac{i.d}{\sigma}$$

Highly conductive electrolytes, such as concentrated KOH in alkaline electrolysers or acidic ionomers in PEM systems, minimize this loss.

2.5.3. Electrode Gap (d)

The distance between anode and cathode (electrode gap) directly affects the ohmic resistance in the cell. A wider gap leads to longer ionic pathways and higher resistive losses:

$$Ro = \frac{d}{\sigma A} \quad ; \quad \eta_o = i.Ro$$

Minimizing the gap helps reduce η_o, but mechanical and design constraints (e.g., membrane thickness, bubble management) limit how close the electrodes can be placed.

2.5.4. Exchange Current Density (i_0)

Exchange current density is a kinetic parameter representing the rate of electron transfer at equilibrium (no net current flow). It dictates how easily electrochemical reactions begin. A higher i_0 implies faster kinetics and lower activation overpotentials, as seen in the Tafel equation (used for approximation in high-overpotential regimes:

$$\eta_{act} = \frac{RT}{\alpha n F} \ln \frac{i}{i_0}$$

Systems with high i_0, achieved via optimized catalysts (e.g., Pt, IrO_2), exhibit superior performance at lower voltages. [31]

2.6. Solar-Powered Electrolysis

2.6.1. Pathways for Solar-Driven Hydrogen Production

Solar energy can drive water electrolysis via three main pathways, each involving a different level of system integration between solar energy harvesting and water splitting: Photovoltaic (PV) Electrolysis, Photo-electrochemical (PEC) Water Splitting and Photochemical Water Splitting. [10]

2.6.1.1. Photo-electrochemical (PEC) Water Splitting

In PEC systems, light absorption and electrochemical water splitting occur in the same component, typically a photo-electrode submerged in an aqueous electrolyte. This photo-electrode is made from a semiconductor material (e.g. TiO_2, Fe_2O_3) that absorbs sunlight and directly generates the necessary voltage to split water into H_2 and O_2. When the energy from the visible light is absorbed, electrons are excited, creating electron-hole pairs (h^+). The excited electrons move toward the cathode, while the electron holes stay at the anode where they oxidize water producing oxygen (O_2), protons (H^+), and electrons (e^-): [32]

Anode: $2H_2O + 4h^+ \rightarrow O_2 + 4H^+$

The electrons at the cathode then combine with protons (H^+) forming hydrogen gas (H_2):

Cathode: $4H^+ + 4e^- \rightarrow 2H_2$

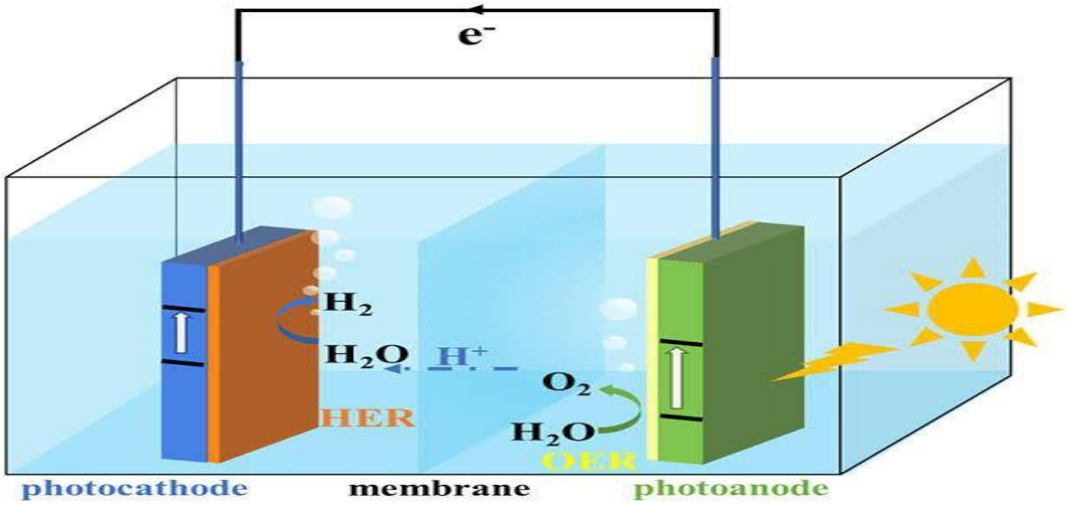

Figure 2.6: PEC Cell[33]

Overall Reaction: $2H_2O$ + *light energy* ➔ $2H_2 + O_2$

PEC does not require an external voltage source, making it more direct and potentially simpler solar-to-hydrogen conversion process. However, despite their conceptual elegance, PEC systems currently suffer from limited efficiencies (typically <5%) and poor long-term stability due to material degradation in aqueous environments. Research is ongoing into stable, earth-abundant semiconductor materials.

2.6.1.2. Photochemical Water Splitting

Photocatalytic water splitting is a promising solar-to-hydrogen conversion method that uses light-sensitive materials to directly catalyse the decomposition of water into hydrogen and oxygen. Unlike PEC systems that require an external circuit, photo-catalysis occurs entirely within suspended particles or films, allowing simpler system designs. The core components in this method are semiconductor photo-catalysts capable of absorbing light and initiating redox reactions in aqueous environments. Various materials have been explored for this purpose, including wide-bandgap semiconductors such as TiO_2, transition metal oxides, and layered metal compounds like $K_4Nb_6O_{17}$, $K_2La_2TiO_{10}$, and Sr_2TaO_7. Additionally, compounds responsive to visible light such as CdS and Cu-ZnS are under active investigation. When exposed to light, these materials generate electron–hole (e^-–h^+) pairs. In TiO_2, for example, UV light with a wavelength below 387 nm excites electrons from the valence band to the conduction band, leaving behind holes. These charge carriers drive the redox reactions: holes oxidize water molecules to produce oxygen, while electrons reduce hydrogen ions in the electrolyte to form hydrogen gas[34].

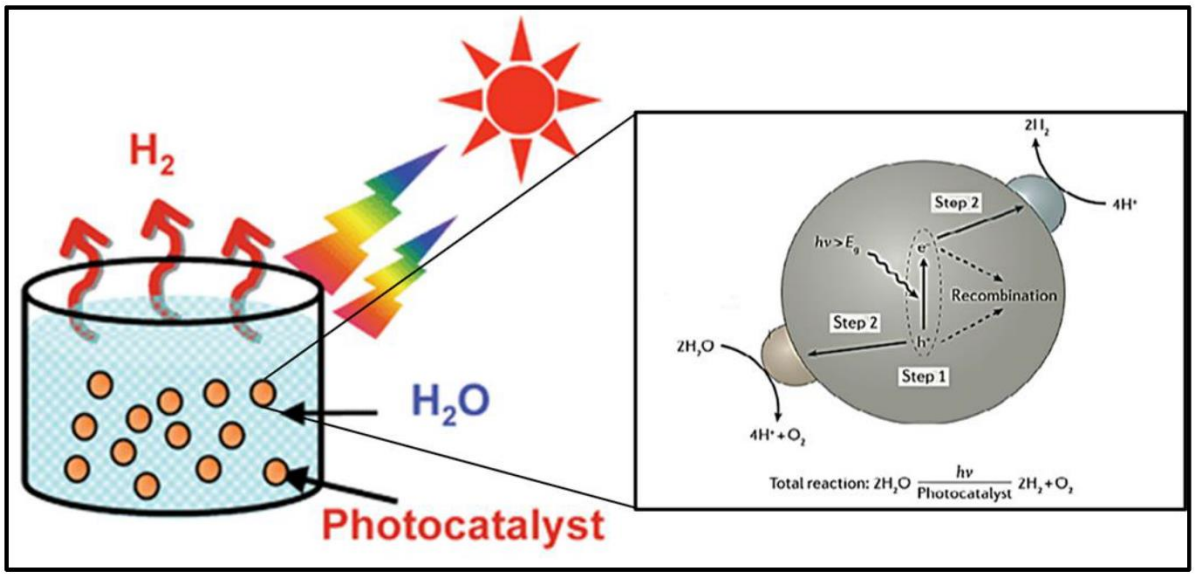

Figure 2.7: Photo-chemical water splitting[34]

Photocatalytic water splitting is conceptually similar to PEC systems, but the reactions in photo-catalysis occur entirely within photoactive semiconductor particles, which act as microscopic photo-electrodes suspended in water. In many systems, both oxidation and reduction reactions take place on the same particle. However, the recombination of photo-generated electron–hole pairs is a significant challenge, limiting efficiency. To suppress these losses, hole scavengers (electron donors) such as certain organic compounds are introduced to consume the holes, allowing electrons to more efficiently reduce protons to hydrogen. This principle opens an innovative pathway where wastewater treatment can be coupled with solar hydrogen production, as many organic pollutants serve as effective hole scavengers. Thus, photo-catalysis holds the potential to address energy and environmental challenges simultaneously. Despite its potential, the practical solar-to-hydrogen (STH) efficiency of photocatalytic systems remains very low—typically around 1–2%. Improving charge separation, extending visible-light responsiveness, and developing co-catalysts remain active research areas aimed at overcoming these performance limitations.

2.6.1.3. PV-Electrolysis

Unlike PEC or photochemical routes, PV-driven electrolysis decouples light absorption from the electrochemical reaction. In this architecture, solar energy is first converted into electricity via photovoltaic panels, which then power a separate electrolyser, typically of the Alkaline or PEM type, as described earlier in Section 2.3.

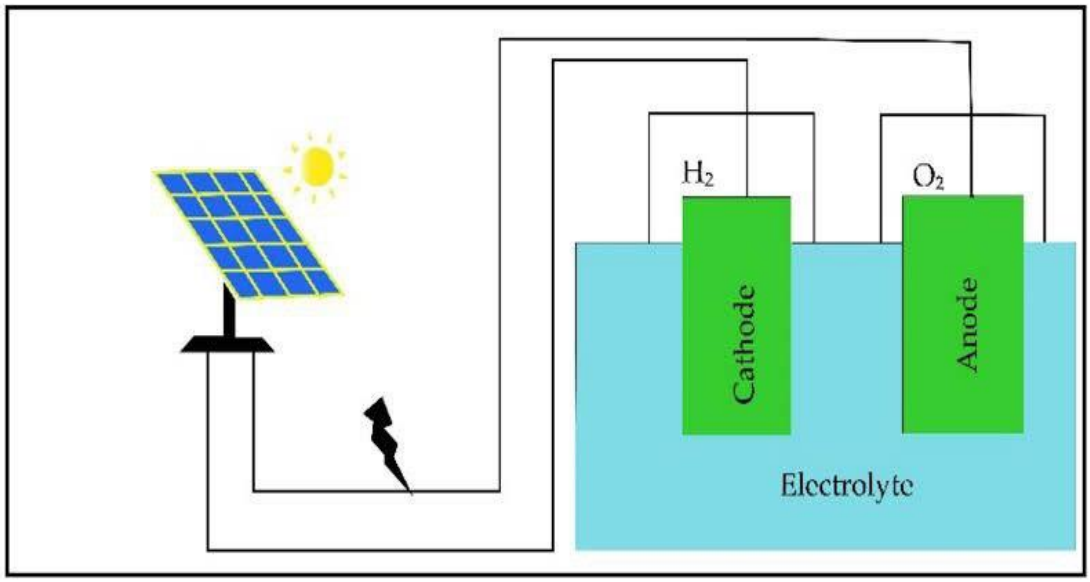

Figure 2.8: PV-Electrolysis setup[35]

This modular approach allows for independent optimization of each subsystem and benefits from the commercial maturity of both PV technology and water electrolysers. System designs can vary based on how the PV array is coupled to the electrolyser:

2.6.1.3.1. Direct coupling:

The PV array powers the electrolyser without intermediate electronics, requiring close voltage-current matching.[36]

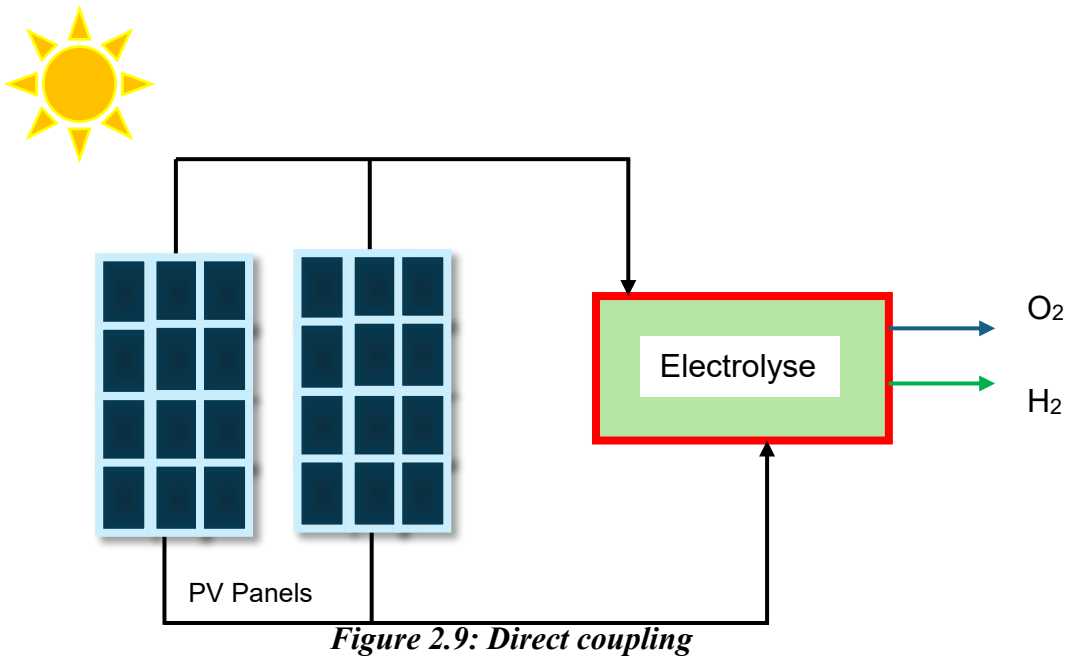

Figure 2.9: Direct coupling

2.6.1.3.2. Indirect coupling:

Includes a power conditioning system (e.g. DC/DC converters or batteries) to stabilize voltage and improve control. The setup is shown in the diagram below:[36]

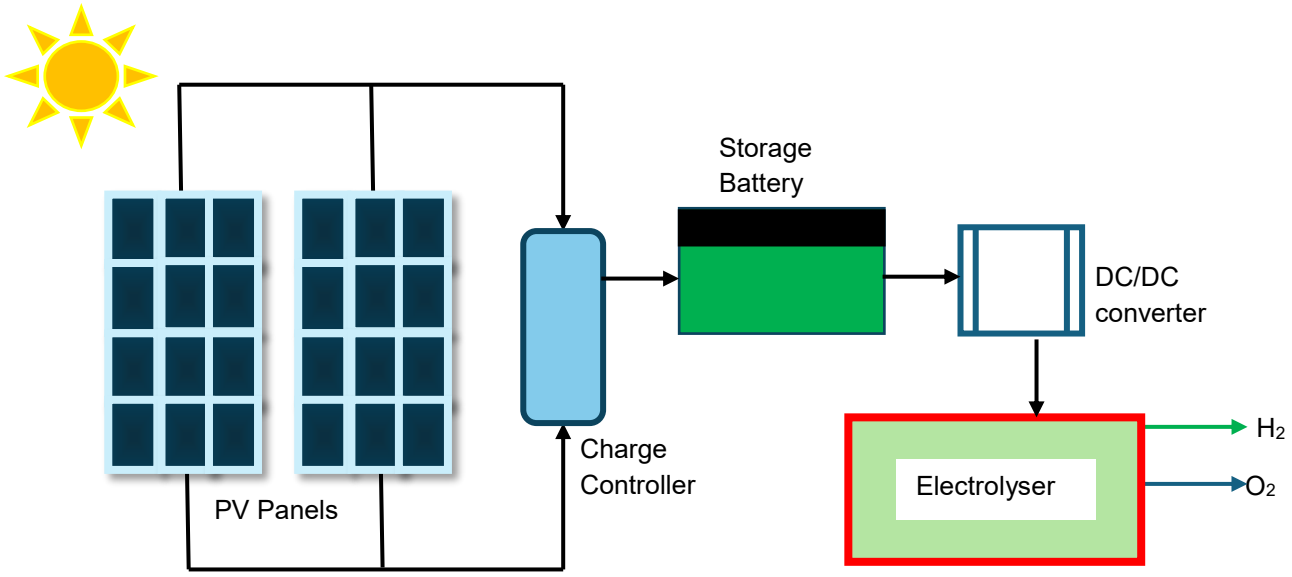

Figure 2.10: Indirect coupling

Among the three pathways for solar hydrogen production, PV electrolysis is currently the most mature and commercially viable route due to its higher efficiencies, ease of component integration, and lower system complexity. In contrast, PEC and photochemical systems are still largely in the research phase, with significant challenges in stability, material cost, and scale-up.

2.6.2. Algeria's Solar Potential

Algeria is enriched with one of the highest solar energy potentials globally, receiving annual solar irradiance levels ranging between 1,700 and 2,600 kWh/m² across most regions. The country's vast Saharan zone, comprising more than 80% of its territory, benefits from over 3,000 hours of sunshine annually, making it highly favourable for large-scale solar-based hydrogen production[37]. In this study, the Aïn Témouchent region was selected as the reference site for modelling solar-powered electrolysis. Located in north-western Algeria, it offers a balance between high solar irradiance and accessibility to infrastructure, water sources, and a moderate climate. Monthly global horizontal irradiance (GHI) and temperature data for Aïn Témouchent were retrieved from the Photovoltaic Geographical Information System (PVGIS) database, ensuring realistic and region-specific input parameters for the simulation. The graph below shows the solar irradiation available in Aïn Témouchent throughout the year, peaking in August and supporting high hydrogen yields.

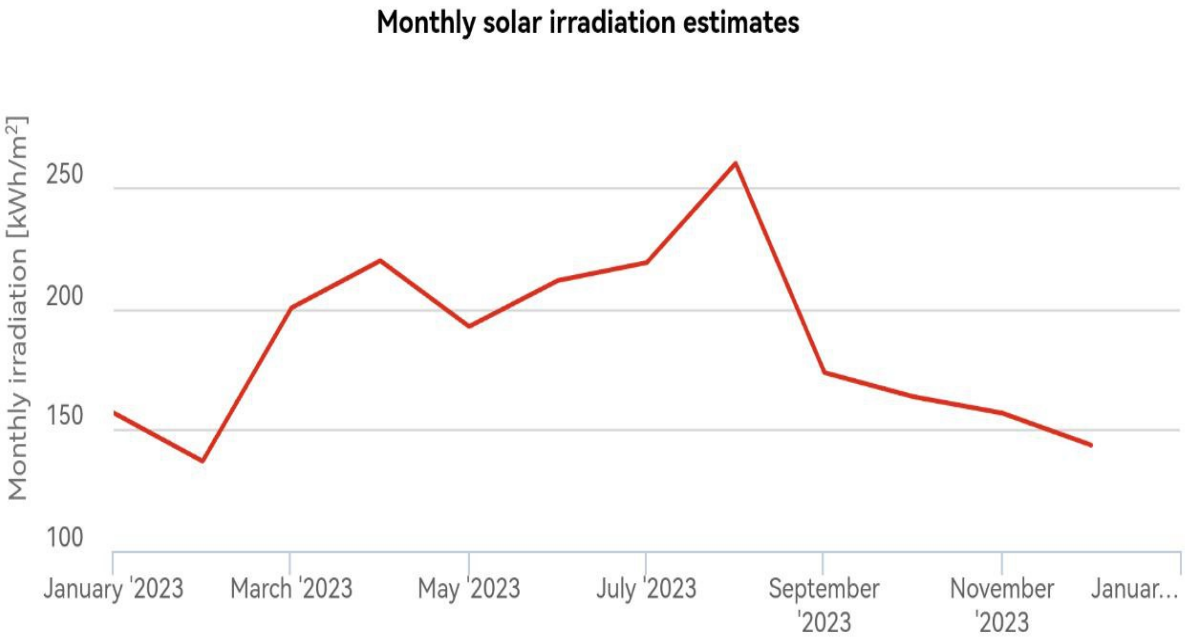

Figure 2.11: Aïn Témouchent's monthly solar irradiation[38]

The profile below shows temperature which is important as it affects both PV efficiency and solar kinetics.

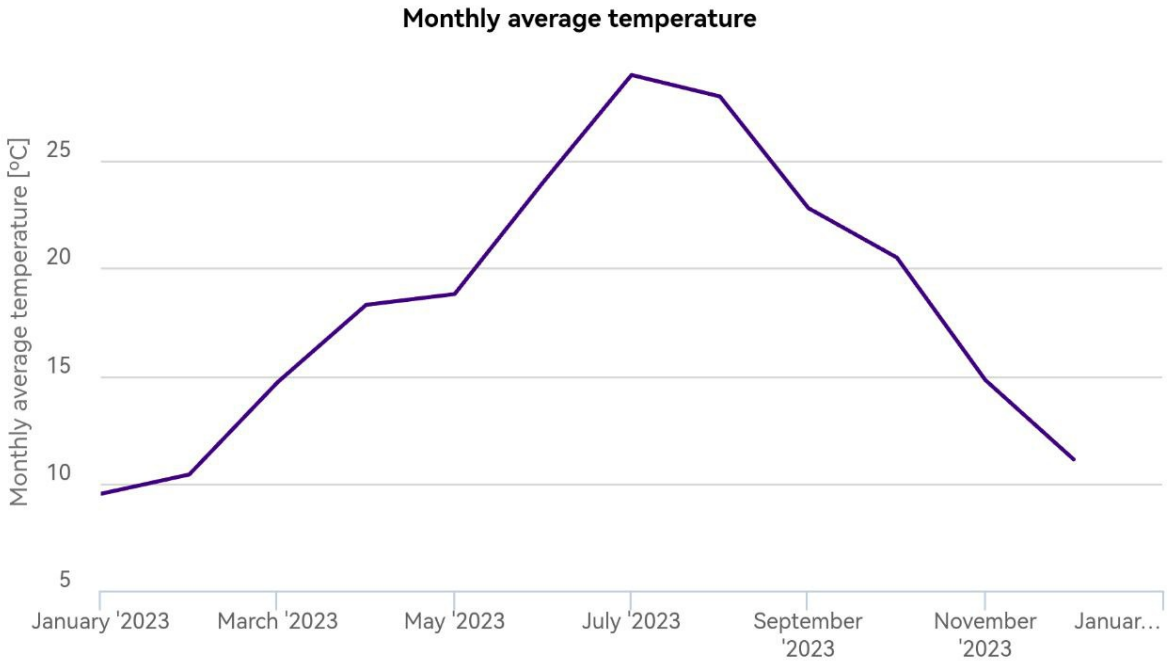

Figure 2.12: Aïn Témouchent's monthly average temperature[38]

This projection shown below, based on system parameters, validates the viability of year-round hydrogen production:

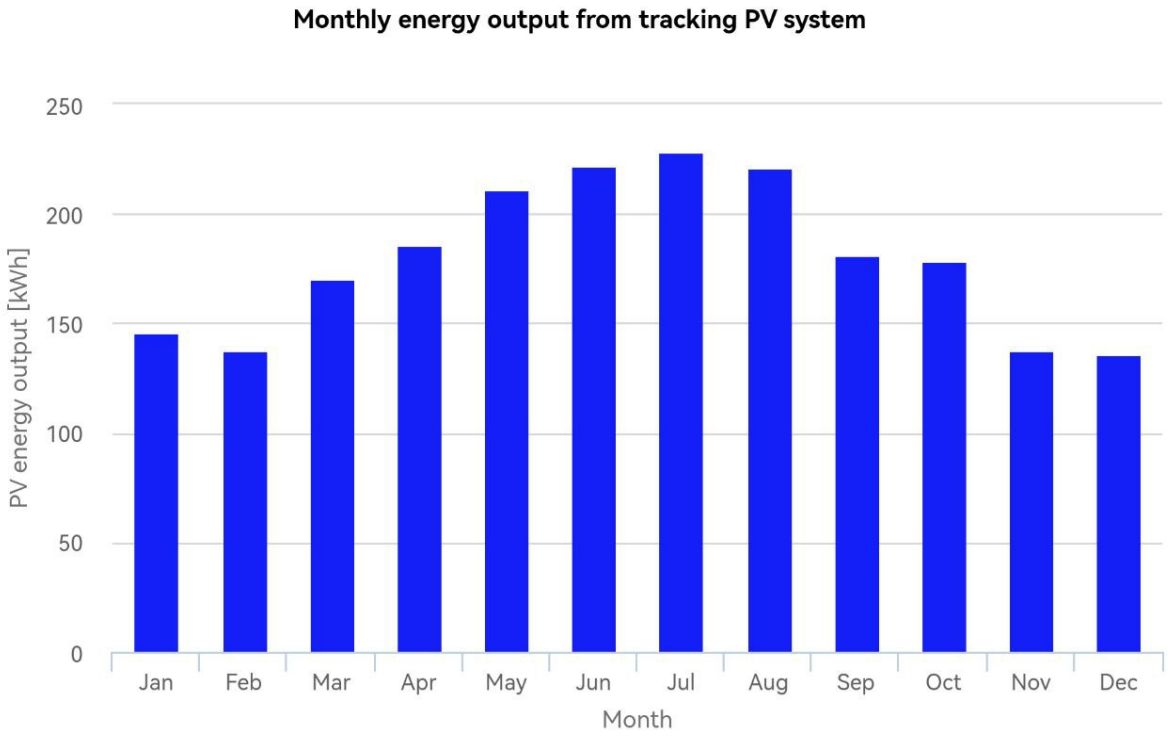

Figure 2.13: Aïn Témouchent's PV energy output for a year[38]

The selection of Aïn Témouchent also aligns with national strategies promoting renewable energy deployment along Algeria's northern and central corridors, where grid access and urban-industrial integration are more feasible. Using this location strengthens the model's practical relevance and highlights the viability of decentralized green hydrogen production in semi-urban Algerian zones.

2.7. Cost and Economic Parameters

Evaluating the feasibility of green hydrogen production from solar energy requires a comprehensive understanding of capital investment, operational costs, and resource availability. This section outlines the theoretical framework and modelling assumptions used to estimate costs, focusing on Capital Expenditure (CAPEX), Operational Expenditure (OPEX), electricity cost derived from solar energy, and water availability scenarios. These assumptions underpin the economic analysis later presented in Chapter 3 of the results.

2.7.1. CAPEX and OPEX

In economic evaluation for the viability of green hydrogen production, two principal cost categories are considered: capital expenditures (CAPEX) and operational expenditures (OPEX). [39]

2.7.1.1. CAPEX:

This refers to the one-time investment costs required to build the system, including the purchase and installation of electrolysers, photovoltaic (PV) panels, power electronics, and water purification units. It also typically includes civil works, grid interconnection, and commissioning costs. Total system CAPEX varies by scale and technology but generally falls within 1000-2500 €/kW of electrolyser capacity in 2023, with expectations to decline toward 500-1000 €/kW by 2030 due to scale and technological learning. [21]

2.7.1.2. OPEX:

This refers to the recurring costs associated with operating and maintaining the system over its lifetime. These may involve labour, scheduled maintenance, component replacement, insurance and administrative costs. In some configurations, the cost of electricity (if imported) and water treatment also contributes to OPEX. It typically falls within the range of 2-4% of total CAPEX per year.

2.7.1.3. Annualization Using CRF

To allow a fair comparison between systems of different lifetimes and configurations, CAPEX is converted to annual cost using the Capital Recovery Factor (CRF):[40]

$$CRF = \frac{r(1+r)^n}{(1+r)^n - 1}$$

Where r is the annual discount rate, commonly 6-10%; n is the project lifetime (15-25years). The annualized CAPEX becomes:

$$Annualized\ CAPEX = Total\ CAPEX * CRF$$

This annualized value is combined with OPEX for total yearly cost estimation.

2.7.1.4. Economies of Scale

In addition, this project incorporates economies of scale through a non-linear cost-scaling relation. As electrolyser system size increases, the specific cost per unit capacity tends to decrease due to bulk purchasing, learning effects, and better utilization of infrastructure. This is modelled by:

$$CAPEX_{scaled} = CAPEX_{ref}\left(\frac{S}{S_{ref}}\right)^{\beta}$$

Where S is the installed system capacity, $CAPEX_{ref}$ is the cost at reference size S_{ref}, and β is the scale factor, typically less than 1. This scaling law captures real-world cost trends observed in larger renewable hydrogen projects and plays a key role in estimating the Levelized Cost of Hydrogen (LCOH), especially under different deployment scales simulated in Chapter 3.[41]

2.7.2. Electricity Cost (LCOE from PV)

The Levelized Cost of Electricity (LCOE) represents the average cost of generating 1 kWh of electricity over the lifetime of a power generation system, accounting for both capital and operational costs. It is a widely used metric in techno-economic assessments of renewable energy systems due to its simplicity and comparability across technologies.

The general expression of LCOE used in literature is:[39]

$$LCOE = \frac{(CAPEX * FCR) + OPEX}{AEP_{net}/1000}$$

Where:

CAPEX is the capital cost per kW of installed capacity (€/kW),

FCR (CRF) is the Fixed Charge Rate, a function of the discount rate and project lifetime,

CAPEX is the annual operational expenditure per kW (€/kW/year), including maintenance, operation, and land costs,

AEP_{net} is the net annual energy production (MWh/year), the denominator converts MWh to kWh for consistency in €/kWh units.

According to IRENA (2023), recent global benchmarks for utility-scale PV systems show LCOE values typically between 0.02–0.06 €/kWh depending on location, scale and technology. In high-irradiance regions like Algeria, the LCOE can fall near the lower end of this range due to strong solar potential and decreasing PV costs, making solar-powered hydrogen production increasingly competitive.[27]

2.7.3. Water Cost and Availability Options

Water is a vital input in electrolysis, and its cost and availability significantly affect the practicality of green hydrogen production, particularly in arid regions. It is typically consumed at 9-10 litres per kg of hydrogen produced. In Algeria, three water sources are considered: freshwater, desalinated seawater, and municipal wastewater. Each presents unique trade-offs in terms of availability, treatment requirements, and associated cost. Freshwater is the most straightforward option, requiring minimal pre-treatment. However, here in Algeria, where fresh water is scarce, its use for industrial electrolysis raises sustainability concerns. Treated seawater, although abundant, requires energy-intensive desalination processes, increasing both capital and operating costs. These costs are typically tied to reverse osmosis systems and depend on local infrastructure. Wastewater presents a promising opportunity for integrated water treatment and hydrogen

production, particularly in urban or industrial zones. Though it requires filtration and possible disinfection, its use promotes circular resource utilization and may lower costs if co-located with treatment plants.[37]

2.7.4. Levelized Cost of Hydrogen (LCOH)

The Levelized Cost of Hydrogen provides a single metric to express the cost of producing one kilogram of hydrogen over the system's lifetime:[41]

$$LCOH = \frac{Annualized\ CAPEX + Annual\ OPEX}{Annual\ Hydrogen\ Production\ (kg)}$$

More detailed models also account for:

$$LCOH = \frac{(\ CAPEX * CRF) + OPEX + Water\ Cost + Electricity\ Cost}{Total\ Hydrogen\ Output\ pear\ year\ \ (kg)}$$

Current literature places LCOH for PV-electrolysis systems between 5–12 €/kg H_2 (small-scale, 2023), 2–5 €/kg H_2 (large-scale, high-irradiance regions like Algeria), with targets to reduce below 1.5 €/kg by 2030[3], [7].

2.8. Conclusion

Electrolytic hydrogen production, powered by renewable energy, is a cornerstone of the green hydrogen economy. This chapter detailed electrolysis principles, including thermodynamic requirements (e.g., minimum voltage of 1.23 V) and key technologies: alkaline, PEM, and solid oxide electrolysers, each with distinct trade-offs in efficiency, cost, and scalability. Losses due to overpotentials (activation, ohmic, concentration) and Faradaic and energy efficiency were analysed, emphasizing the need for optimized operational parameters such as electrode gap and conductivity. Solar-powered electrolysis pathways, PEC, photochemical, and PV-electrolysis were evaluated, with PV-electrolysis identified as the most mature for large-scale deployment. Algeria's high solar potential (GHI ~2,000 kWh/m²/year) positions it favourably for green hydrogen projects. Economic analysis introduced CAPEX/OPEX considerations, LCOE of PV and Levelized Cost of Hydrogen (LCOH), highlighting economies of scale and renewable energy affordability as critical drivers. The chapter concludes that system integration, material advancements, and policy support are essential to make solar-driven electrolysis commercially viable.

3 Chapter 3: Results and Discussion

3.1. Introduction

This chapter presents the results of the PV-powered electrolysis simulation conducted for Aïn Témouchent, Algeria. The aim for this simulation is to quantify hydrogen production potential, assess system efficiency and evaluate the cost of hydrogen generation. A MATLAB-based model was developed using real monthly solar irradiance and temperature data for the city of Aïn Témouchent taken from the Photovoltaic Geographical Information System (PVGIS) database, the simulation incorporates electrochemical and economic sub-models. Key parameters include a PV area of 500 m², Faradaic efficiency of 90%, and standard electrochemical performance metrics. Results are presented through monthly and hourly profiles, parametric sweeps, and a final optimized comparison.

3.2. Electrolyser sizing

The goal here is to find the area of the electrolyser (A_{cell}) that is compatible with the PV power generated.

3.2.1. PV data from PVGIS database

Hourly PV data including temperature and irradiance for the whole year 2023 was gathered from the PVGIS database and from this data we picked the highest value for the irradiance (G_{peak}) and the highest temperature (T_{peak}). The irradiance was at a peak of 1138.1 W/m^2 at 12:09 in the month of March and the temperature was at a peak of 42.5°C at 14:09 in July. The information is presented in the graph below:

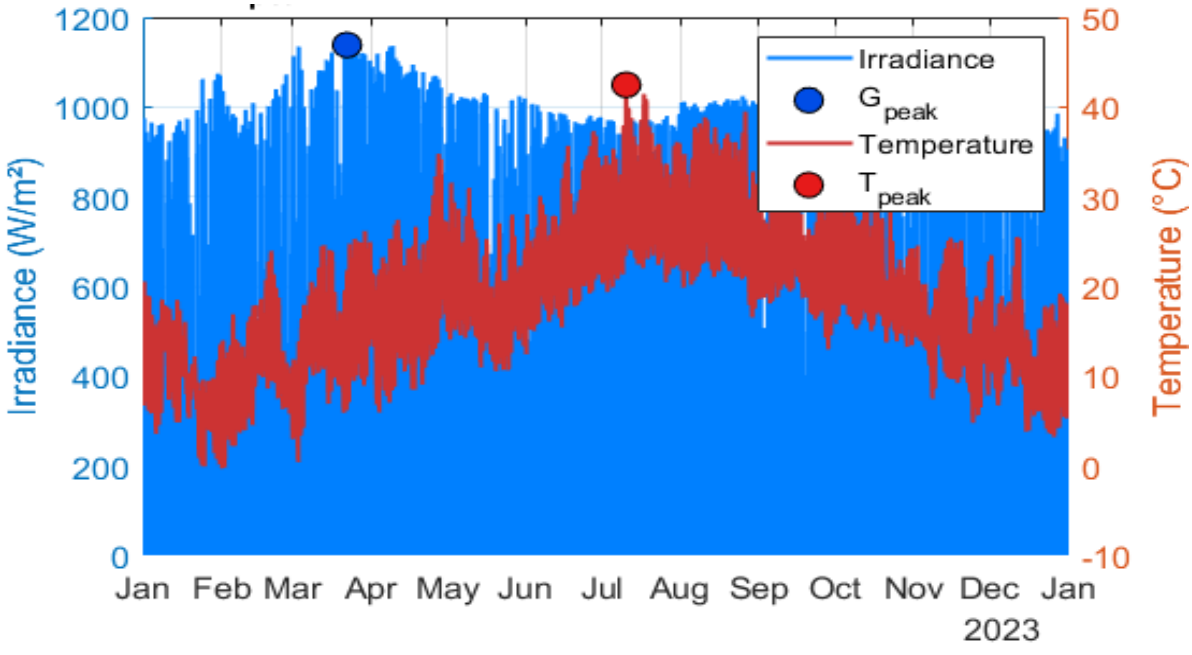

Figure 3.1: Irradiance and temperature peak values

Now with the peak values for irradiance and temperature known, we are able to find the maximum power that our PV solar can generate and therefore the required electrolyser area that can handle that power.

3.2.2. Calculating the electrolyser area (A_{cell})

All the parameter values for the calculation of A_{cell} are shown in the table below:

Parameter	Value
Peak irradiance (G_{peak})	1138.1 W/m^2
Peak ambient temperature ($T_{Amb\text{-}peak}$)	42.5 °C
Target current density ($J_{nominal}$)	4000 A/m^2
Typical voltage ($V_{nominal}$)	1.9V
PV area (A_{PV})	500 m^2
η_{PV}	0.18

Table 3.1: Input parameters for the electrolyser sizing

- Temperature efficiency

$$\eta_{T_{Amb-peak}} = \eta_{PV} * (1 - 0.003 * (T_{Amb-peak} - 25))$$

$$\eta_{T_{Amb-peak}} = 0.1706$$

- Power [W]

$$P_{peak} = G_{peak} * A_{PV} * \eta_{T_{Amb-peak}}$$

$$P_{peak} = 97065\ W$$

- Current [A]

$$I_{peak} = \frac{P_{peak}}{V_{nominal}}$$

$$I_{peak} = 51087\ A$$

- Electrolyser area [m^2]

$$A_{cell} = \frac{I_{peak}}{J_{nominal}}$$

$$A_{cell} = 12.7718\ m^2$$

3.3. PV calculations

$\eta_{Temp} = \eta_{PV} * (1 - 0.003 * (T_{amb} - 25))$; 0.003 is the temperature coefficient at 25°C

$\eta_{Temp} = 0.2292$

$E = G_d * A_{PV} * \eta_T$

$E = 691.265$ kWh

Gd is the daily irradiance and Tamb is the daily ambient temperatures.

$$P_{avg} = \frac{E_{kWh}*1000}{PSH} = \frac{E_{kWh}*1000}{6.11}$$

$$P_{avg} = 113140\ W$$

- Note

PSH (Peak Sun Hours) is defined as 1 hour of sunlight at 1000 W/m^2 (1 kWh/m2), that is 1 PSH = 1 kWh/m2

For one month we have:

$$PSH_i = \frac{Monthly\ Irradiation}{Number\ of\ days\ in\ the\ month}$$

For example, for January we have:

$$PSH_i = \frac{156.75}{31} = 5.06\ kWh/m^2/day$$

Therefore for all the 12 months we have:

$$PSH = \frac{\sum_{i=1}^{12} PSH_i}{12} = \frac{73.31}{12} = 6.11\ kWh/m^2/day = 6.11\ hours/day$$

3.4. Electrolyser calculations

Parameter	Value
Faraday constant	96485 C/mol
Universal gas constant (R)	8.314 J/mol.K
Molar mass of hydrogen (M_{H2})	2.016 * 10^{-3} kg/mol
Faraday efficiency (η_F)	0.9
Operating Temperature (T)	80 °C
Electrolyte Conductivity Temperature Coefficient (α)	0.02 $°C^{-1}$
Electrolyte Conductivity at 25 °C (K_{25})	55 S/m
Electrode gap	0.002 m
Number of cells	1
OER (Anode) Exchange current density (J0-anode)	0.3 A/m^2
Anode charge transfer coefficient (α_{anode})	0.5
HER (Cathode) Exchange current density (J0-cathode)	5 A/m^2
Cathode charge transfer coefficient ($\alpha_{cathode}$)	0.5

Table 3.2: Input parameters for the electrolyser calculations

3.4.1. Adjusting parameters to the operating temperature

Since the alkaline electrolyser was operated at 80 °C, the parameters have to be scaled to fit the operating temperature

3.4.1.1. Electrolyte Conductivity at 80 °C

$$K_T = K_{25} * (1 + \alpha * (T - 25))$$

$$K_{80} = K_{25} * (1 + \alpha * (80 - 25)) = 115.5\ S/m$$

- Ohmic Resistance :

$$R = \frac{d}{K_{80}} = 1.7316 * 10^{-5}\ \Omega.m^2$$

3.4.1.2. Reversible voltage at 80 °

$$E_{rev}(T) = 1.5184 - 1.5421 * 10^{-3}T + 9.523 * 10^{-5}\,T\ln(T) + 9.84 * 10^{-8}\,T^2$$

$$E_{rev}(T) = 1.1834\ V$$

3.4.2. Cell Voltage Estimation and Hydrogen Production Calculation

To simulate the electrochemical performance of the electrolyser, a step-by-step voltage estimation routine was performed. This method calculates the actual operating cell voltage (V_{cell}) under varying average power inputs by accounting for all relevant electrochemical losses. Firstly, an initial estimate of the cell voltage ($V_{cell,est}$) is used to estimate the total current:

$$I_{total} = \frac{P_{avg}}{V_{cell,est}}$$

Then, the current density is determined by dividing the total current by the active electrode area:

$$J = \frac{I_{total}}{A_{cell}}$$

This current density is used to calculate each overpotential component:

Activation overpotentials at the anode and cathode are computed using the Butler-Volmer equation:

$$J = J_0 \left[exp\left(\frac{\alpha F \eta}{RT}\right) - exp\left(-\frac{(1-\alpha)F\eta}{RT}\right)\right]$$

To ensure computational efficiency, the Newton-Raphson method was used with an initial value of the activation overpotential derived from the inverse hyperbolic sine approximation:

$$\eta_{act,initial} = \frac{RT}{\alpha F} sinh^{-1}\left(\frac{J}{2J_0}\right)$$

Ohmic losses are calculated from the product of current density and the total electrical resistance:

$$\eta_{ohm} = J * R$$

Concentration overpotential is included using a logarithmic expression that considers the limiting current density (J_{limit} = 10 000 A/m^2):

$$\eta_{conc} = \frac{RT}{2F}\, ln\left(\frac{J_{limit}}{J_{limit} - J}\right)$$

The total cell voltage is then calculated as:

$$V_{cell} = E_{rev(T)} + \eta_{act,a} + \eta_{act,c} + \eta_{ohm} + \eta_{conc}$$

This process is repeated iteratively, updating the value of Vcell,est until the value converges within a tolerance of 10^{-6}V or a maximum of 50 iterations.

Once the final cell voltage is determined for a given day, it is then used to calculate the total electrical charge delivered:

$$Q = \frac{E_{kWh} * 3.6 * 10^6}{V_{cell}}$$

This charge is then used to compute the mass of hydrogen produced daily using Faraday's law:

$$m_{H_2} = \frac{Q * \eta_F}{2F} * M_{H_2}$$

All the output data of the calculations above is shown in the table below:

Parameter	Value
Total current (I_{total})	50445 A
Current density (J)	3283.7 A/m^2
Anode activation overpotential ($\eta_{act,a}$)	0.5733 V
Cathode activation overpotential ($\eta_{act,c}$)	0.4061 V
Ohmic overpotential (η_{ohm})	0.0684 V
Concentration overpotential (η_{conc})	0.0076 V
Operating cell voltage (V_{cell})	2.2428 V
Electrical charge (Q)	110.9 * 10^6 C
Mass of H_2 produced (m_{H2})	About 2-14 kg/day

Table 3.3: Output values including H_2 production and V_{cell}

3.5. System Performance Analysis

3.5.1. Hydrogen Output

The simulated annual hydrogen output under baseline conditions was 3169.8 kg. Figure 1 displays monthly production trends, with the highest yields in July and the lowest in December, reflecting seasonal solar irradiance patterns. Summer months saw higher irradiation but also increased temperatures, which slightly reduced PV efficiency.

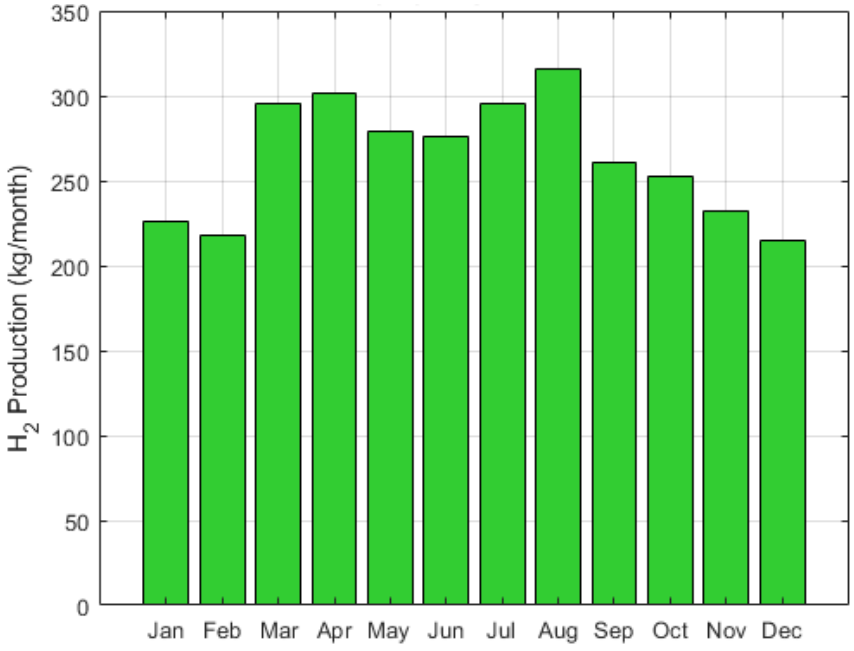

Figure 3.2: Monthly hydrogen production

3.5.2. Electrolyser Performance

The average cell voltage over the simulation period was 2.2 V, fluctuating between 1.93 V and 2.26 V. Figure 3.3 illustrates the hourly voltage profile. Breakdown of average overpotentials includes: activation (anode: 0.5733 V, cathode: 0.4061 V), ohmic (0.0684 V), and concentration (0.0076 V). Figure 3.4 presents the variation of these overpotentials over time, highlighting activation losses as the dominant contributor and the table below it shows the percentage contributed to the overall voltage loss by each overpotential. To complete the electrolyser performance insight, Figure 3.5 shows the hourly variation of the current density.

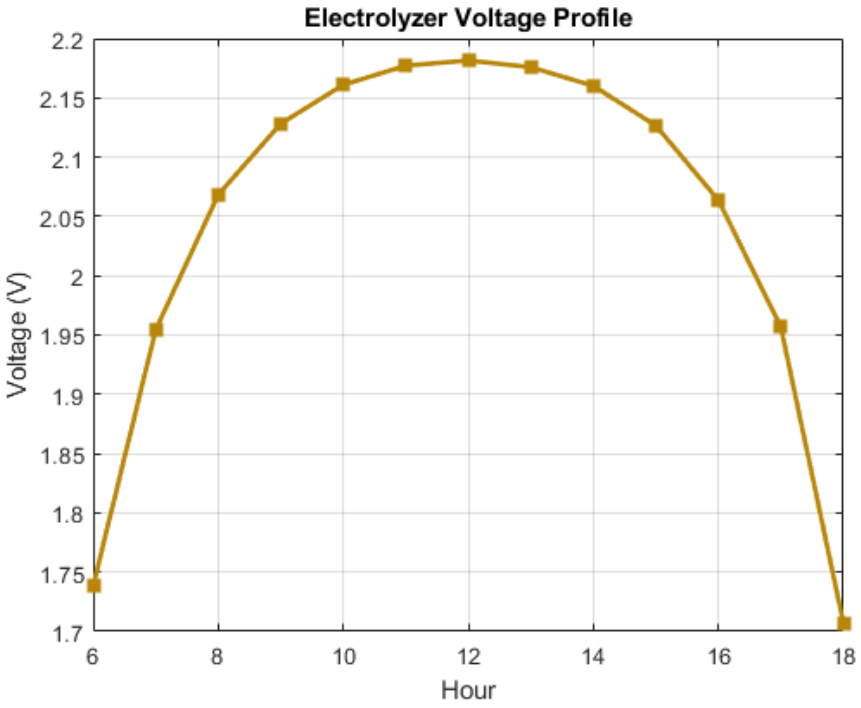

Figure 3.3: Electrolyser cell voltage

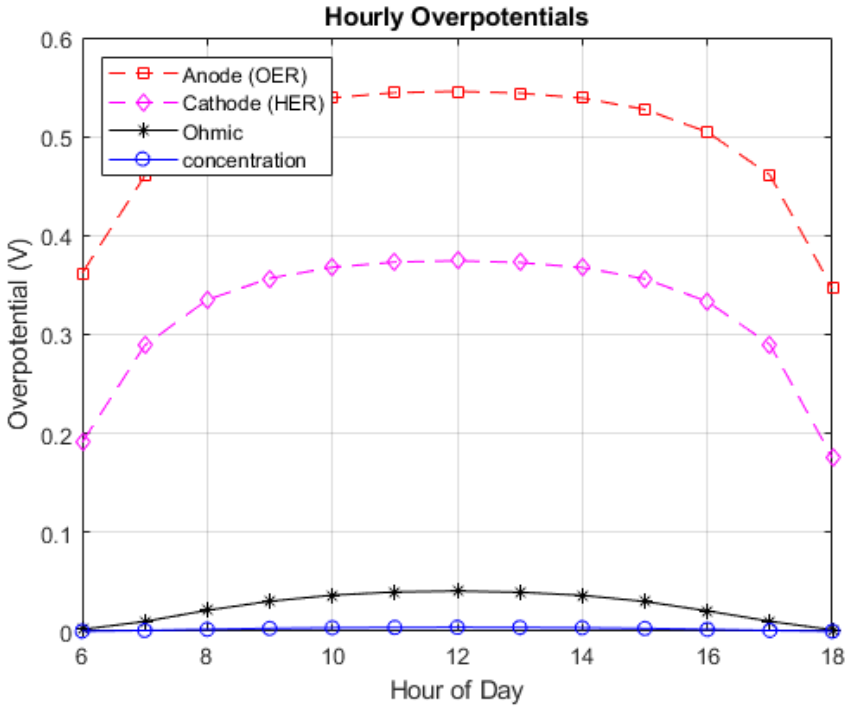

Figure 3.4: Hourly overpotentials for a typical day

Overpotential	% Contribution
Anode activation overpotential ($\eta_{act,a}$)	54.49
Cathode activation overpotential ($\eta_{act,c}$)	38.33
Ohmic overpotential (η_{ohm})	6.46
Concentration overpotential (η_{conc})	0.72

Table 3.4: Overpotentials' percentage contribution to voltage loss

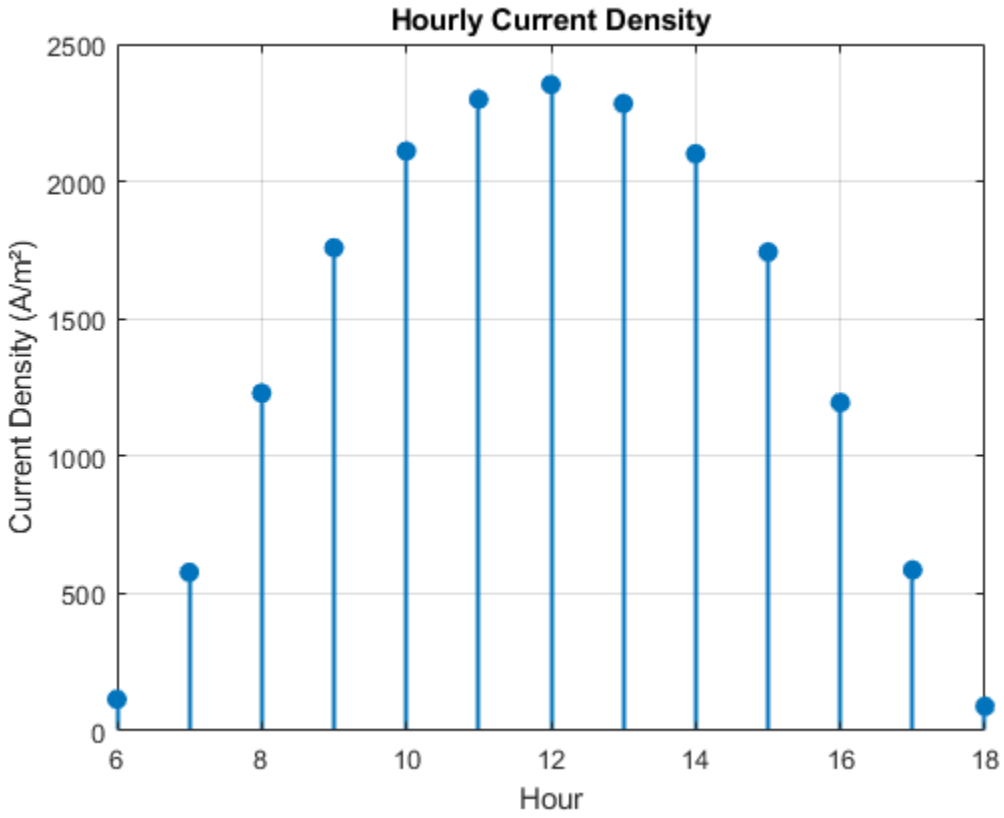

Figure 3.5: Hourly current density

3.5.3. PV System Performance

Hourly PV power generation peaks around midday and follows the solar profile closely. Temperature effects caused slight efficiency reductions during hot hours. Daily energy availability determined the hydrogen production profile, which showed strong correlation with PV power availability. The joint graph of PV power and the amount of hydrogen produced is shown below:

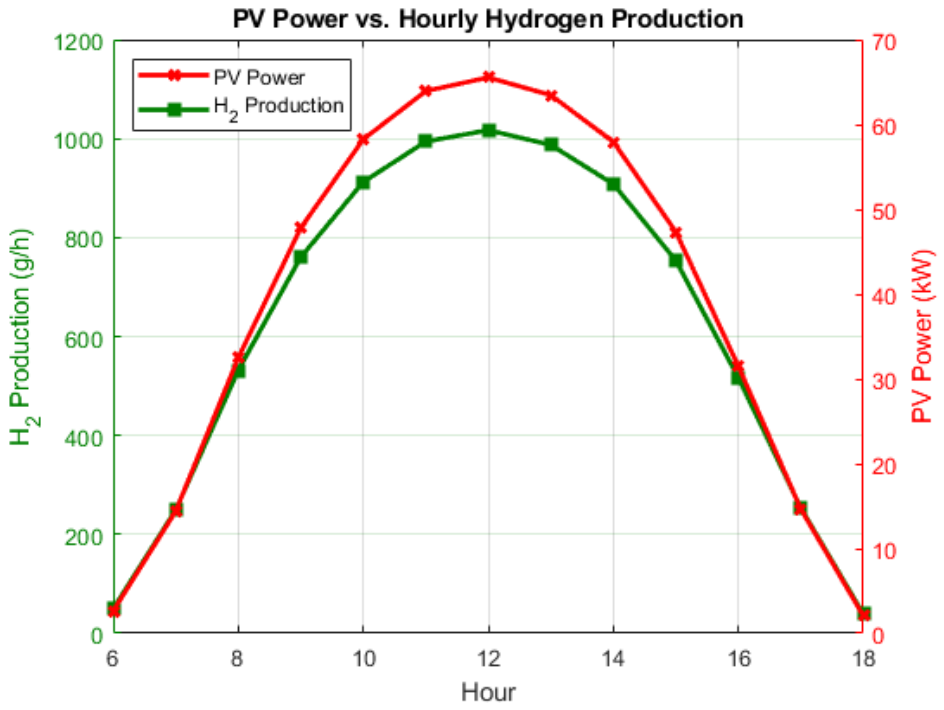

Figure 3.6: Hourly PV power vs hydrogen production

3.6. Economic Analysis

3.6.1. Cost Components

Capital expenditures (CAPEX) for the PV array and electrolyser were scaled based on area and capacity, respectively. Operational expenditures (OPEX) included maintenance and electricity costs. Water consumption, based on 10 L/kg of H_2 plus process losses, contributed to the total cost.

Parameter	Value
PV CAPEX	800 € /kW
Electrolyser CAPEX	1000 € /kW
PV OPEX rate	0.015
Electrolyser OPEX rate	0.03
Lifetime (n)	20 years
Discount rate (r)	0.07
PV scale factor (β_{PV})	0.9
Electrolyser scale factor (β_{Elec})	0.8
Base area (A_{base})	50 m^2
PV Area (A_{PV})	50 – 500 m^2
Water cost	0.5 €/m^3

Table 3.5: Input values used in the economic analysis

- Capital Recovery Factor:

$$CRF = \frac{r(1+r)^n}{(1+r)^n-1} = 0.0944$$

- Scaled CAPEX per kW:

$$CAPEX_{PV,scaled} = CAPEX_{PV} * \left(\frac{A_{PV}}{A_{base}}\right)^{\beta pv-1} = 635.4626 \text{ €/kW}$$

$$CAPEX_{Elec,scaled} = CAPEX_{Elec} * \left(\frac{A_{PV}}{A_{base}}\right)^{\beta Elec-1} = 630.9573 \text{ €/kW}$$

- CAPEX total:

$$CAPEX_{PV,total} = P_{peak} * CAPEX_{PV,scaled} = 65091€$$

$$CAPEX_{Elec,total} = P_{peak} * CAPEX_{Elec,scaled} = 64\,629 €$$

$$CAPEX_{total} = CAPEX_{PV,total} * CAPEX_{Elec,total} = 129720 €$$

- Annualized Capital Recovery Cost:

$$CAPEX_{recovery} = CAPEX_{total} * CRF = 12245 €$$

- Annual Operating Expenditures:

$$OPEX_{annual} = CAPEX_{total} * \left(r_{OPEX,PV} + r_{OPEX,Elec}\right) = 5837.4 €$$

- Water cost:

The amount of water consumed annually is:

$$Water\ Consumed_{Annual} = m_{H2,Annual} * Water_{kg/kgH2}$$

$$Water\ Consumed_{Annual} = 31\,698kg = 31761\ l$$

The annual water cost is then:

$$Water\ Cost_{Annual} = \ Water\ Consumed_{Annual} * \ Water\ Cost_{per\ kg} = 15.8492€$$

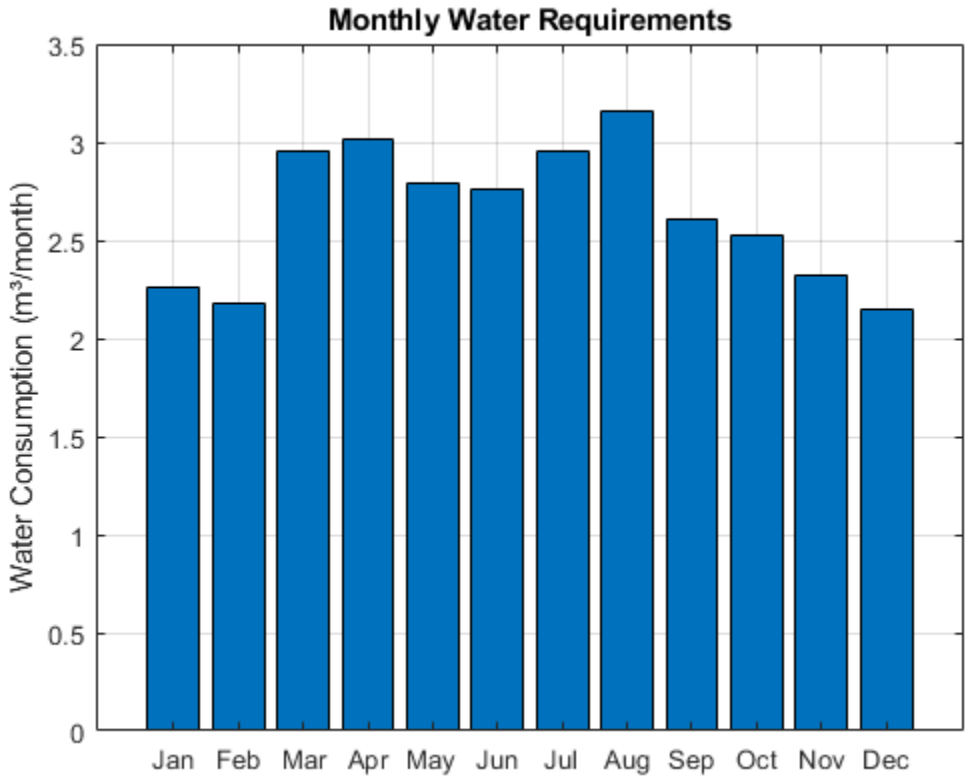

Figure 3.7: Monthly water requirements

- The total annual cost is therefore:

$$Cost_{annual,total} = \ OPEX_{annual} + \ CAPEX_{recovery} + \ Water\ Cost_{annual}$$

$$= 18098\ €$$

3.6.2. Levelized Costs

The baseline Levelized Cost of Electricity (LCOE) was 0.056 €/kWh. Resulting hydrogen production cost was 5.71 €/kg.

- LCOE:

$$LCOE = \frac{CAPEX_{PV,total} + CRF + OPEX_{annual}}{E_{annual}} = 0.056\ €/kW$$

- Hydrogen production cost:

$$Cost_{H2} = \frac{Cost_{annual,total}}{m_{H2,annual}} = 5.71 \text{ €/kg}$$

Figure 3.8 details how increasing PV area (50–500 m²) impacts annual hydrogen production and cost, demonstrating economies of scale.

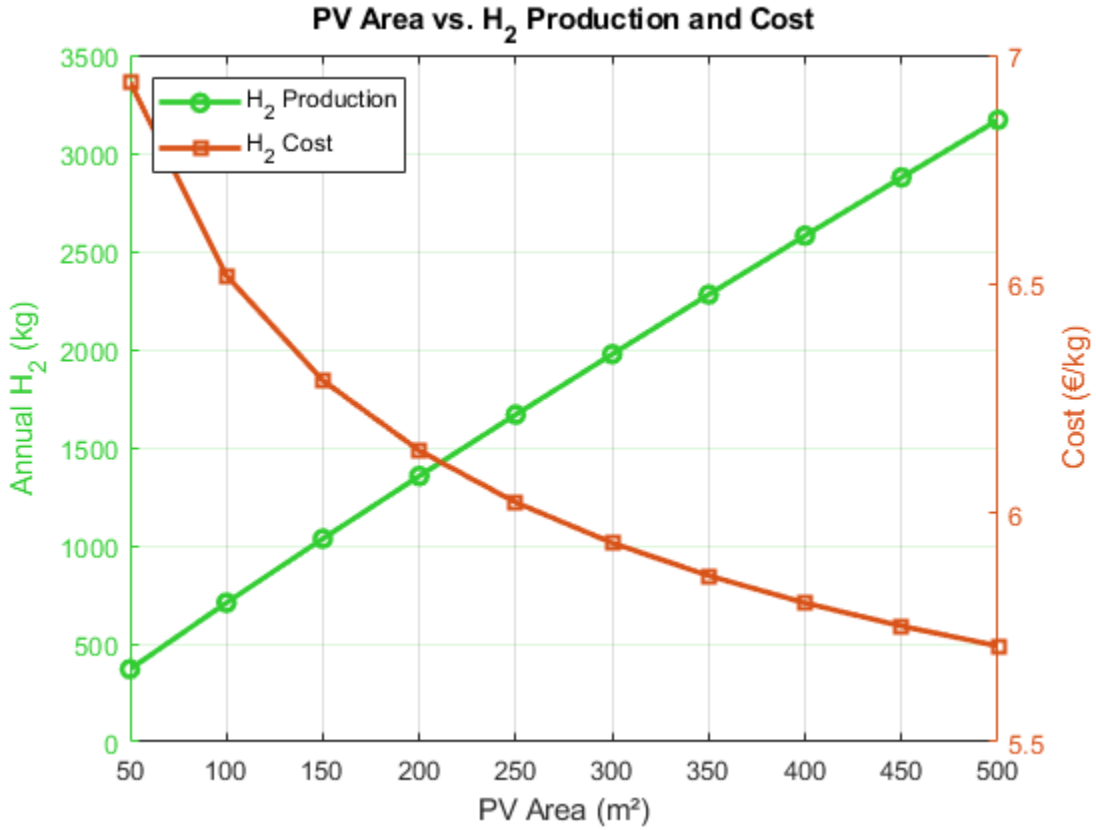

Figure 3.8: PV area vs hydrogen production and cost

Month	Irradiance (W/m^2)	Temperature (°C)	PV Energy (kWh)	H^2 Produced (kg)	Production Cost (€)	Water Consumed (m^3)
Jan	208.9	9.2926	13988	226.46	1293	2.2646
Feb	224.18	10.381	13559	218.01	1244.7	2.1801
March	282.23	14.321	18898	295.65	1688	2.9565
April	301.37	18.177	19529	301.45	1721.1	3.0145
May	268.97	18.838	18010	279.32	1594.8	2.7932
June	279.4	23.836	18105	276.51	1578.7	2.7651
July	293.15	28.907	19629	295.06	1684.6	2.9506
August	314.77	28.052	21077	315.86	1803.4	3.1586
September	262.13	22.936	16986	261.02	1490.3	2.6102
October	242.98	20.623	16270	253	1444.5	2.53
November	226	14.858	14645	232.57	1327.9	2.3257
December	198.3	11.606	13278	214.93	1227.1	2.1493

Table 3.6: Monthly Performance Summary

3.7. Parametric Studies and Sensitivity Analysis

To identify these most influential parameters affecting hydrogen production and cost, we performed a three-step process: single-parameter variations, sensitivity analysis, and a combined optimisation using the top two parameters.

3.7.1. Single Parameter Variations

Five parameters were varied individually across 10 values within a common and realistic range, while keeping all parameters constant. The parameters tested were:

1)

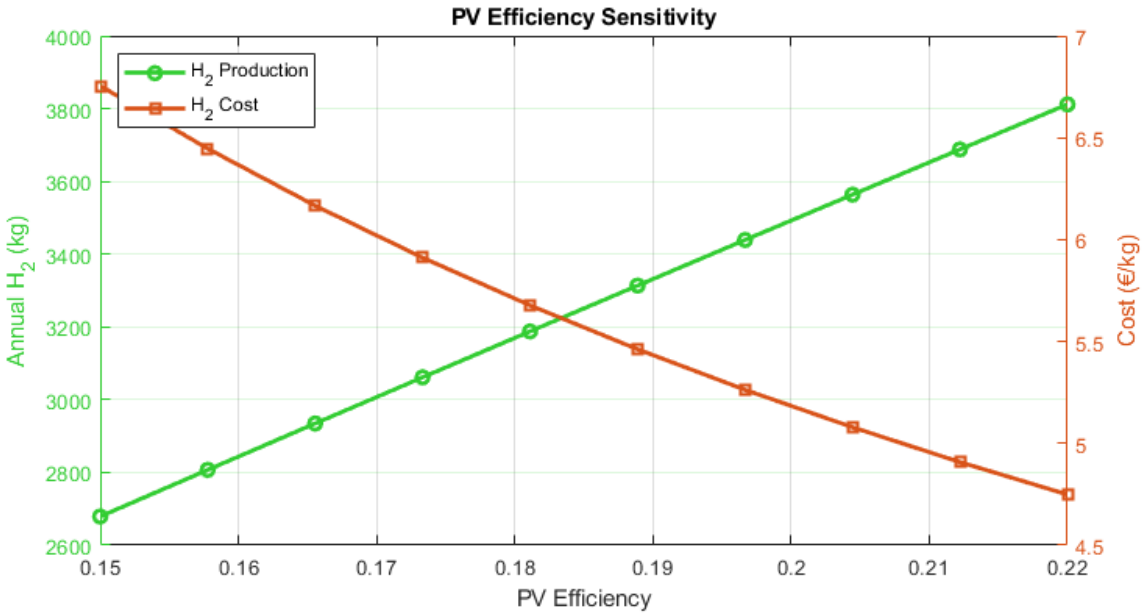

Figure 3.9: Faradaic Efficiency (0.85–0.95)

2)

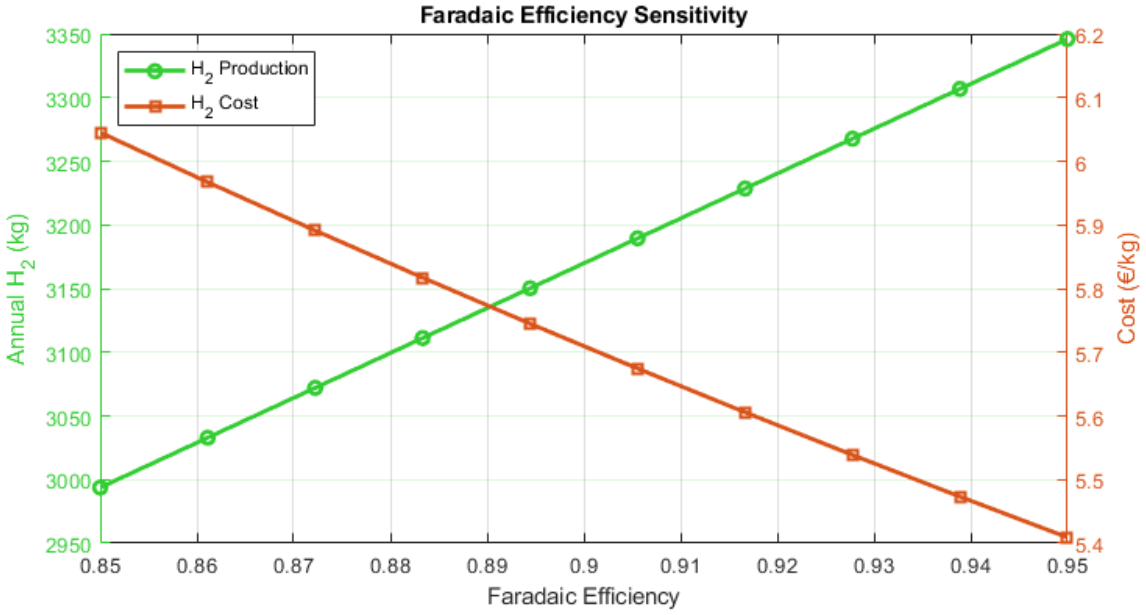

Figure 3.10: PV Efficiency (15%–22%)

3)

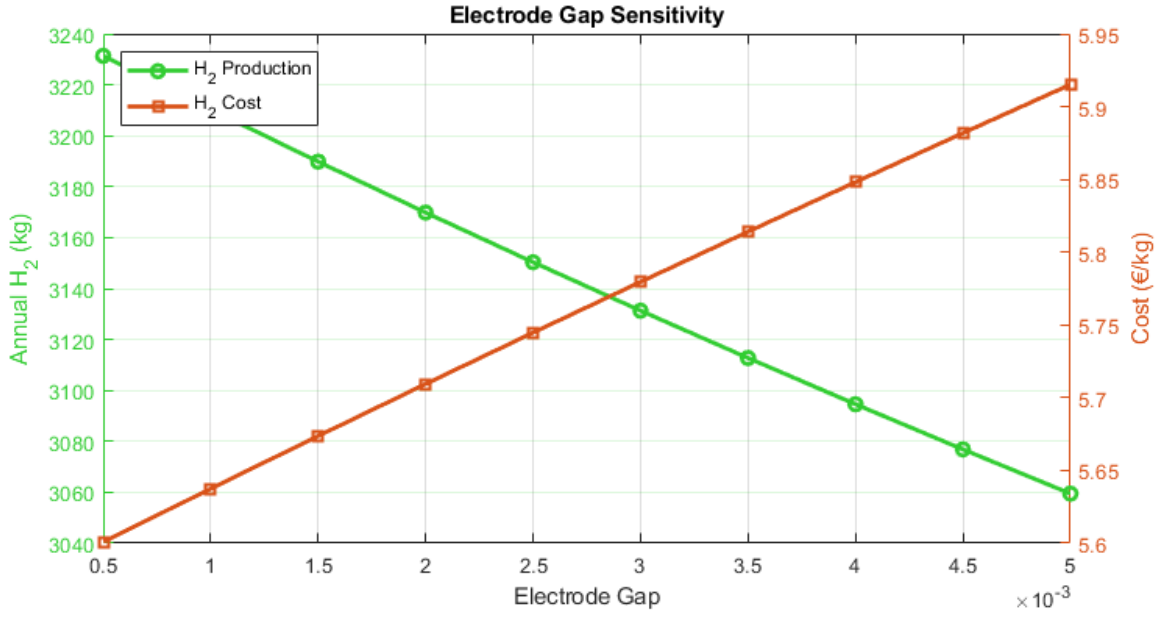

Figure 3.11: Electrode Gap (0.5–5 mm)

4)

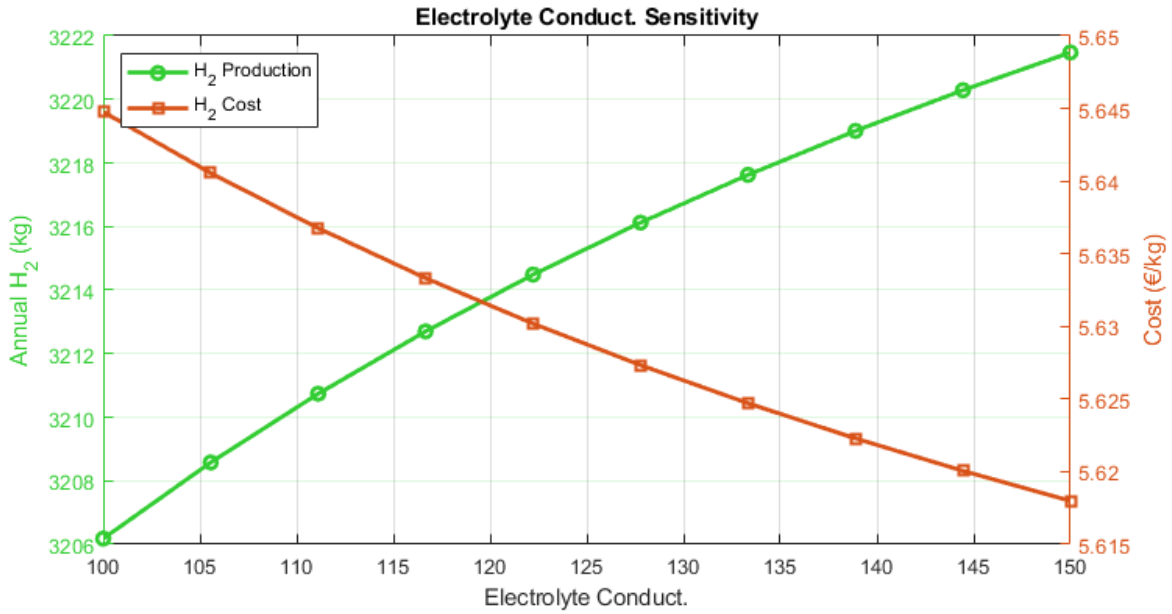

Figure 3.12: Electrolyte Conductivity (100–150 S/m)

5)

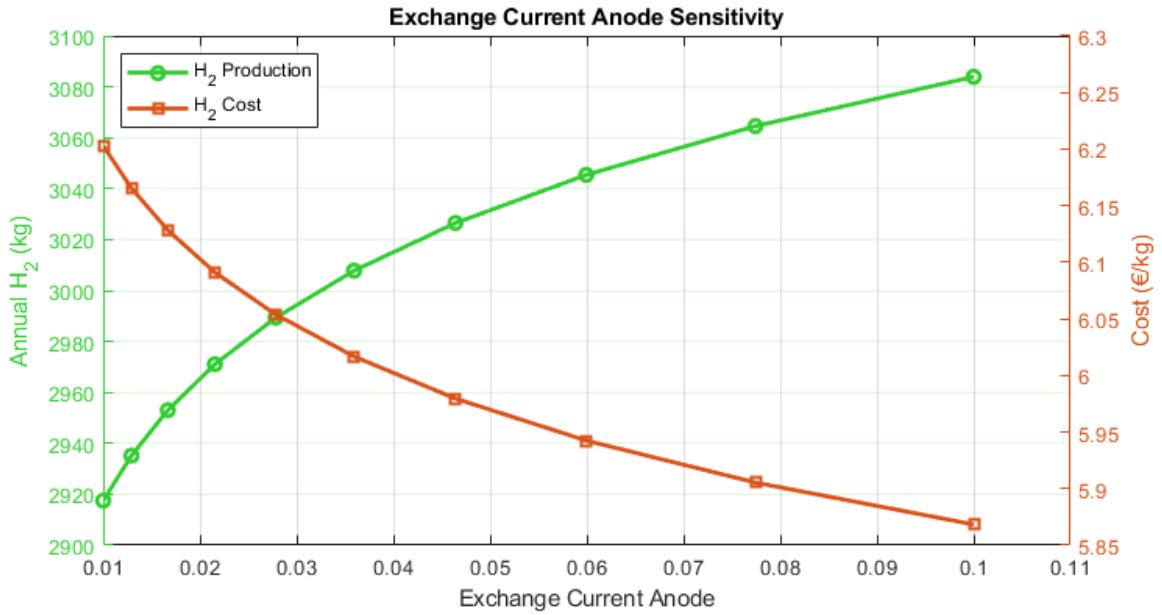

Figure 3.13: Exchange Current Density (0.01–0.1 A/m²)

3.7.2. Sensitivity Analysis

To quantify the influence of each parameter on hydrogen yield, a sensitivity coefficient was calculated:

$$S = \frac{(H_{max} - H_{min})/H_{min}}{(P_{max} - P_{min})/P_{min}}$$

Where H is hydrogen production and P is the tested parameter. This formulation gives the fractional change in hydrogen output per fractional change in the input parameter. The top two parameters with the highest positive sensitivities were Faradaic Efficiency and PV Efficiency, which were then selected for multi-variable optimization.

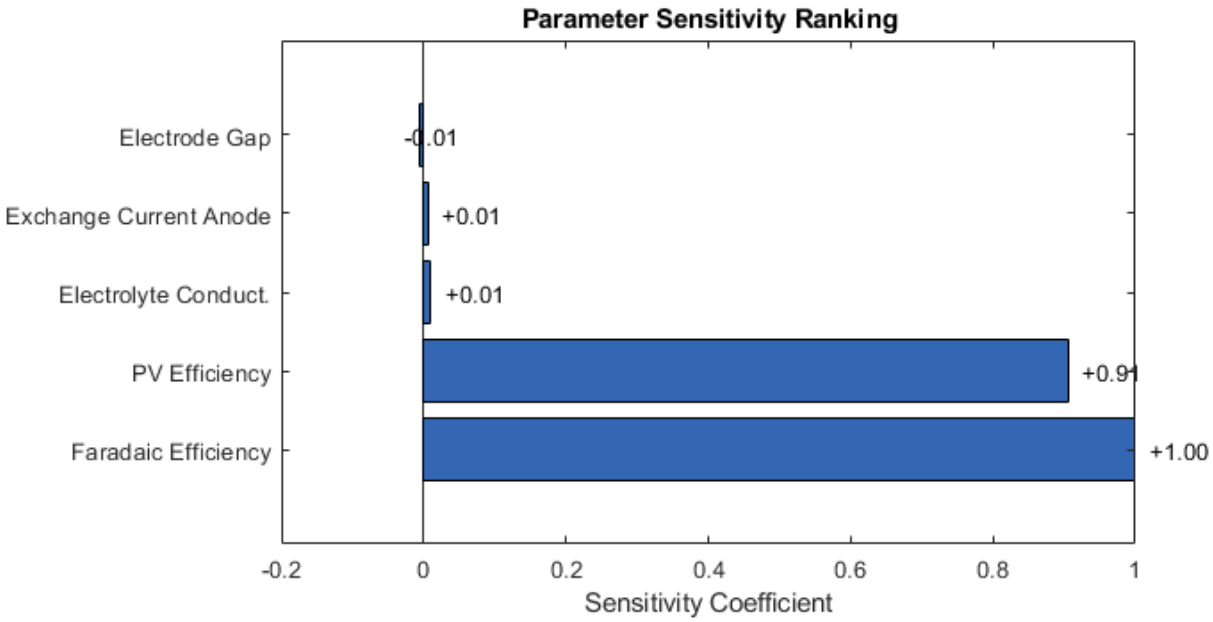

Figure 3.14: Parameter sensitivity ranking

3.7.3. Combined Two-Parameter Optimization

A 2D parameter grid was created using the top two sensitive variables. Both were varied simultaneously across 5 evenly spaced values within their respective ranges. This yielded a 5×5 matrix of simulation runs. For each combination, the annual hydrogen output and hydrogen cost were recorded. The resulting surfaces allow visualization of the interaction between PV and Faradaic efficiency, and help identify the region of optimal performance. The surface plots illustrated the joint influence of Faradaic efficiency and PV efficiency on hydrogen production and cost. The optimal configuration (Faradaic efficiency = 0.95, PV efficiency = 0.22) yielded 4023.5 kg/year at 4.50 €/kg.

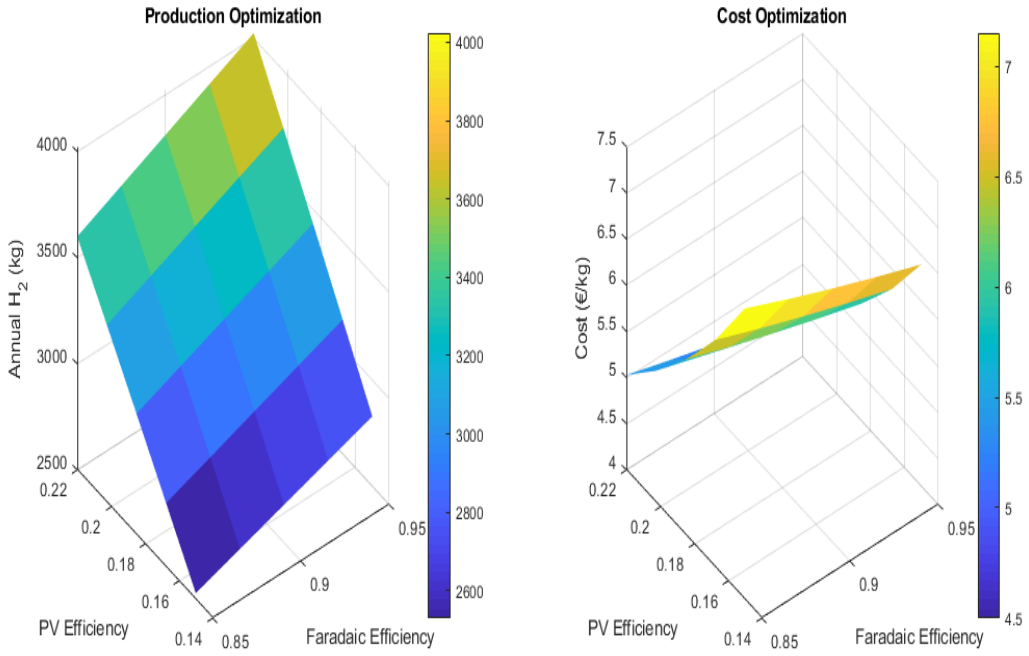

Figure 3.15: 2D parameter grid of hydrogen production and cost optimization

3.7.4. Baseline vs. Optimized Comparison

To evaluate the effectiveness of the optimization process, key performance indicators (KPIs) from the original (baseline) model were compared against the results obtained through 2D parameter optimization involving PV efficiency and Faradaic efficiency.

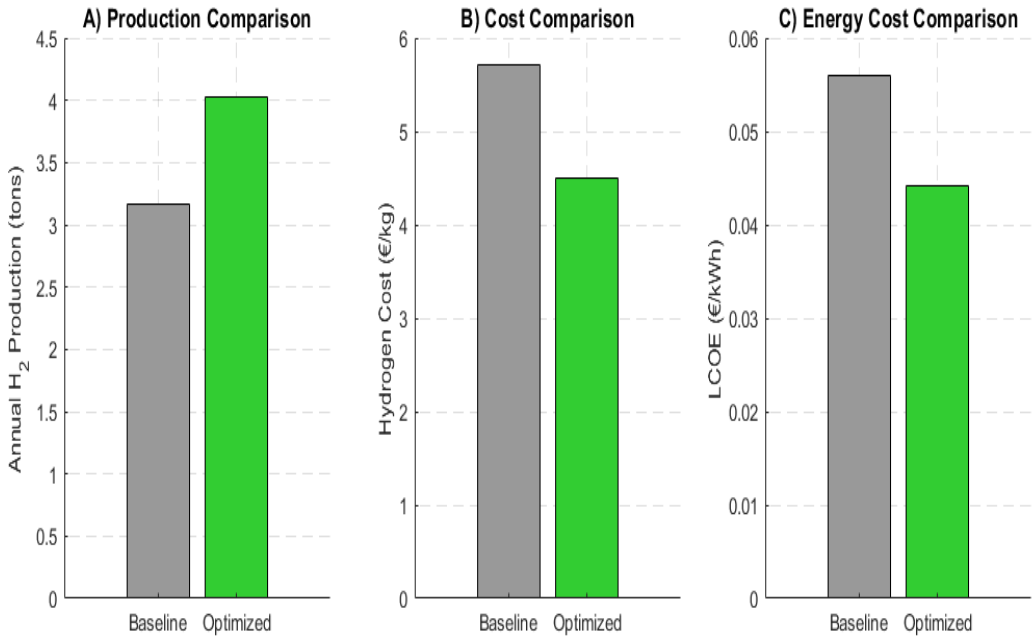

Figure 3.16: Baseline vs optimized model comparison

	Baseline	Optimized	Improvement
Annual H2 Produced (kg)	3169.8	4023.5	+26.9%
H2 Production Cost (€)	5.71	4.50	+21.2%
Water Consumed (m3)	31.7	40.2	+26.9%
LCOE (€/kWh)	0.056	0.044	+21.2%

Table 3.7: Summary of the baseline and optimized model outputs

3.8. Conclusion

This chapter employed a MATLAB simulation to model a solar-powered electrolysis system in Ain Temouchent, Algeria, integrating PV performance data, electrolyser sizing, efficiency calculations and economic feasibility. The PVGIS data revealed peak irradiance of 1,138.1 W/m² and the maximum ambient temperature of 42.5°C, leading to an electrolyser area of 12.77 m² to match the PV output of 131.14 kW average daily power. The MATLAB simulation of the alkaline electrolyser at an operating temperature of 80°C, achieved optimized parameters, including an electrolyte conductivity of 115.5 S/m, a reversible voltage of 1.1834 V, and a cell voltage of 2.2428 V, with activation (anode: 0.5733 V, cathode: 0.4061 V), ohmic (0.0684 V), and concentration

(0.0076 V) overpotentials. The current density reached 3 283.7 A/m², demonstrating strong performance under high solar input. Economically, the scaled CAPEX for PV (€635/kW) and electrolyser (€634/kW) totalled €129 720, with annual OPEX of €5,837.4 and water costs of €15.85/year. The baseline LCOH was €5.71/kg H_2, but optimization (Faradaic efficiency = 95%, PV efficiency = 22%) increased annual H_2 production from 3 169.8 kg to 4 023.5 kg, reducing LCOH to €4.50/kg H_2. Sensitivity analysis highlighted Faradaic efficiency (+1.00) and PV efficiency (+0.91) as the most impactful parameters, while electrode gap, electrolyte conductivity and exchange current density had minimal influence. The MATLAB simulation confirms that solar-powered electrolysis via alkaline electrolysers is technically feasible in high-irradiation regions like Algeria, with efficiency dependent on temperature management and overpotential reduction. To enhance competitiveness, focus should be put on scaling electrolyser manufacturing, reducing PV costs and exploring hybrid renewable systems and efforts should be made to integrate advanced electrode materials to enhance alkaline electrolyser performance under renewable power inputs.

4 General Conclusion

In this study we have investigated the potential of green hydrogen production through solar-powered electrolysis, with a specific focus on alkaline electrolyser technology coupled photovoltaic (PV) systems. Our comprehensive analysis, covering fundamental principles, technical modelling and economic assessment confirms that alkaline electrolysers represent a rational and competitive choice for large-scale solar hydrogen production, though with some notable trade-offs compared to alternatives like PEM and solid oxide electrolysers. The research has sufficiently examined green hydrogen production's technical feasibility, economic viability and strategic importance in the global energy transition. As we began with fundamental principles and progressed to detailed case study analysis, we have managed to highlight critical insights into hydrogen's role as a clean energy vector and the practical challenges of its renewable-powered production.

The foundational Chapter 1 established hydrogen as an energy carrier with the potential to decarbonize multiple sectors of the modern economy. Through comprehensive analysis of production methods, we distinguished between conventional fossil-based pathways (grey/blue hydrogen) and emerging renewable approaches (green hydrogen). The chapter highlighted steam methane reforming's current dominance while emphasizing its carbon-intensive nature, contrasted with electrolysis's potential when coupled with renewable electricity. Storage and transportation challenges were examined in depth, revealing compressed gas and cryogenic liquid methods as mature but limited solutions, with promising alternatives like ammonia and liquid organic hydrogen carriers requiring further development. Crucially, this chapter positioned hydrogen as an essential component of deep decarbonization strategies, particularly for hard-to-abate sectors such as heavy industry, long-haul transport, and seasonal energy storage.

Building on these fundamentals, Chapter 2 focused specifically on electrolysis technologies and their integration with solar energy systems. The comparative analysis of Alkaline, PEM and Solid Oxide electrolysers revealed distinct advantages and limitations for each technology. Alkaline systems demonstrated cost advantages for large-scale deployment and also boasts of being the longest existing technology, thus the most mature, while PEM electrolysers showed superior dynamic response characteristics which are valuable for intermittent renewable operation. The detailed examination of overpotentials (activation, ohmic, and concentration overpotentials), provided critical insights into efficiency limitations, with the Butler-Volmer equation analysis quantifying these losses. Solar integration pathways were thoroughly evaluated, with PV-electrolysis emerging as the most immediately viable approach, while photo-electrochemical methods showed long-term potential. Algeria's exceptional solar resources were quantified, with irradiation levels exceeding 2,000 kWh/m²/year creating ideal conditions for solar hydrogen

production. Economic analysis introduced key metrics including CAPEX, OPEX, and levelized cost of hydrogen (LCOH), establishing frameworks for subsequent case study evaluation.

The practical application of these principles was demonstrated in Chapter 3's detailed MATLAB simulation. Using high-resolution PVGIS data for Ain Temouchent, Algeria, the research quantified system performance under real-world conditions. The 12.77 m² electrolyser system, matched to 131.14 kW PV output, achieved notable efficiency at 80°C operation, with electrolyte conductivity of 115.5 S/m and cell voltage of 2.2428 V. The comprehensive overpotential analysis revealed activation losses as the dominant efficiency limitation, suggesting priority areas for future material improvements. Economic assessment yielded baseline LCOH of €5.71/kg, reducible to €4.50/kg through optimization of Faradaic and PV efficiencies. The sensitivity analysis provided particularly valuable insights, identifying Faradaic efficiency (+1.00) and PV efficiency (+0.91) as primary cost drivers, while electrode gap, electrolyte conductivity and exchange current density variations showed minimal impact.

Several critical findings emerge from this integrated analysis. Firstly, solar-powered electrolysis has reached technical maturity for deployment in high-irradiation regions, with current technologies capable of delivering hydrogen at costs approaching competitiveness with fossil-based alternatives. Secondly, the research identifies specific efficiency limitations, particularly activation overpotentials that represent priority targets for materials research and development. Thirdly, the case study demonstrates that regional advantages in solar resources can translate into significant economic benefits for hydrogen production, positioning sun-rich nations like Algeria as potential leaders in the emerging green hydrogen economy.

As we move forward into the future, several pathways emerge for advancing green hydrogen adoption. Technological innovation should focus on catalyst development to reduce activation overpotentials, membrane materials to enhance conductivity, and system designs that maintain efficiency under variable solar input. Economies of scale in both PV and electrolyser manufacturing will be crucial for cost reduction, suggesting the need for coordinated industrial policy. The research also highlights the importance of integrated system design, where synergies between solar generation characteristics and electrolyser operational parameters can optimize overall performance.

Policy implications are significant. The findings support targeted deployment incentives in regions with superior solar resources, coupled with infrastructure development for hydrogen storage and transport. International standards for hydrogen certification will be essential to create transparent markets for green hydrogen. The research also suggests the value of pilot projects demonstrating integrated renewable hydrogen systems at commercial scale.

This study confirms that solar-powered green hydrogen has transitioned from theoretical potential to practical reality. While challenges remain in scaling production and reducing costs, the technical

and economic foundations are now established. For nations like Algeria with abundant solar resources, green hydrogen represents both an environmental imperative and a significant economic opportunity in the emerging clean energy economy. The coming years will be critical for translating this potential into large-scale reality through continued innovation, strategic investment, and supportive policy frameworks.

5 References

[1] IEA, “Global Hydrogen Review,” 2023.

[2] UNECE, “Hydrogen Technology Brief.”

[3] IRENA, “The Energy Progress Report,” 2022.

[4] A. R. Barron, *Chemistry of the main Group Elements*.

[5] J. Jonas, “The History of Hydrogen,” 2009.

[6] IEA, “World Energy Outlook,” 2021.

[7] Hydrogen Council, “Hydrogen Insights,” 2023.

[8] P. Nikolaidis and A. Poullikkas, “A comparative overview of hydrogen production processes,” *Renew. Sustain. Energy Rev.*, vol. 67, pp. 597–611, 2017, doi: 10.1016/j.rser.2016.09.044.

[9] W. L. Jolly, “Hydrogen”.

[10] D. A. Khan et al, *Hydrogen Energy: Production, Storage, and Utilization*.

[11] C. Russu, “The Pros and Cons of Hydrogen as a Decarbonization Instrument,” 2024.

[12] R. Ramachandran and R. K. Menon, “An Overview of Industrial Uses of Hydrogen”.

[13] N. Ghasem, “A Review of the CFD Modeling of Hydrogen Production in Catalytic Steam Reforming Reactors”.

[14] B. Phung et al, “The Current Status of Hydrogen Energy”.

[15] T. E. Lipman and A. Z. Weber, “Fuel Cells and Hydrogen Production”.

[16] Z. Fang et al, “Production of Hydrogen from Renewable Resources”.

[17] A. G. Konstandopoulos, C. Pagkoura, D. A. Dimitrakis, S. Lorentzou, and G. P. Karagiannakis, *Solar Hydrogen Production BT - Production of Hydrogen from Renewable Resources*, vol. 1734. 2015. doi: 10.1007/978-94-017-7330-0_10.

[18] J. Hou and M. Yang, *Green Hydrogen Production by Water Electrolysis*.

[19] A. J. Bard and L. R. Faulkner, *Electrochemical Methods; Fundamentals and Applications*.

[20] A. Godula-Jopek, *Hydrogen Production by Electrolysis*. 2015.

[21] E. Mukiza, “The Effects of Pressure and Temperaure on Alkaline Electrolysis,” LUT University, 2024.

[22] P. Kirsch, “Electrolyser Performance and Degradation under Various Load Shapes”.

[23] A. S. Tijania et al, “Mathematical Modelling and Simulation Analysis of Advanced

Alkaline Electrolyzer System for Hydrogen production".

[24] R. D. Williams, *Hydrogen Energy System.*, vol. 5, no. 3. 1975. doi: 10.2190/0H1K-8GU7-NC5H-1LX0.

[25] L. Zhang et al, *Electrochemical Water Electrolysis Fundamentals and Technologies*. 2020.

[26] R. Lira et al, "Elucidating the Increased Ohmic Resistances in Zero-Gap Alkaline Water Electrolysis".

[27] S. Peng, *Electrochemical Hydrogen Production from Water Splitting*. 2023. doi: 10.1007/978-981-99-4468-2.

[28] N. Sabli et al, "Hydrogen Production by Membrane Water Splitting Technologies".

[29] S. S. Kuma and L. Hankwon, "An Overview of Water Electrolysis Technologies for Green Hydrogen Production".

[30] H. Ouabi et al, "Hydrogen Production by Water Electrolysis Driven by a Photvoltaic Source".

[31] J. O. Bockris, *Modern Electrochemistry*.

[32] H.-J. Lewerenz et al, *Photoelectrochemical Water Splitting: Materials, Processes and Architectures*.

[33] L. Jun et al, "Tandem Nanostructures: A Prospective Platform for Photoelectrochemical Water Splitting".

[34] M. Mohsin et al, "Semiconductor nanmaterial Photocatalysts fo Water-Splitting Hydogen Production".

[35] A. K. Sarker et al, "Prospects of Green Hydrogen Generation from Hybrid Renewable Energy Sources".

[36] T. L. Gibson et al, "Optimization of Solar Powered Hydrogen Using Photovoltaic Electrolysis Devices".

[37] Y. Benchenina et al, "Directions, Advancing Green Hydrogen In Algeria with Opportunities and Challenges for Future."

[38] PVGIS, "Ain Temouchent PV Data," 2023. https://re.jrc.ec.europa.eu/pvg_tools/en/tools.html

[39] C. Mone et al, "Cost of Wind Energy Review".

[40] TIO Markets, "Capital Recovery Factor Explained," 2024.

[41] EHO, "Levelised Cost of Hydrogen Calculator Manual," *2024*.